USDA Forest Service
U.S. DEPARTMENT OF AGRICULTURE

General Technical Report WO-109a | June 2026

Forest Health Monitoring: Evaluation Monitoring Project Summaries 2024

EDITORS: Simone Lim-Hing and Karun Pandit

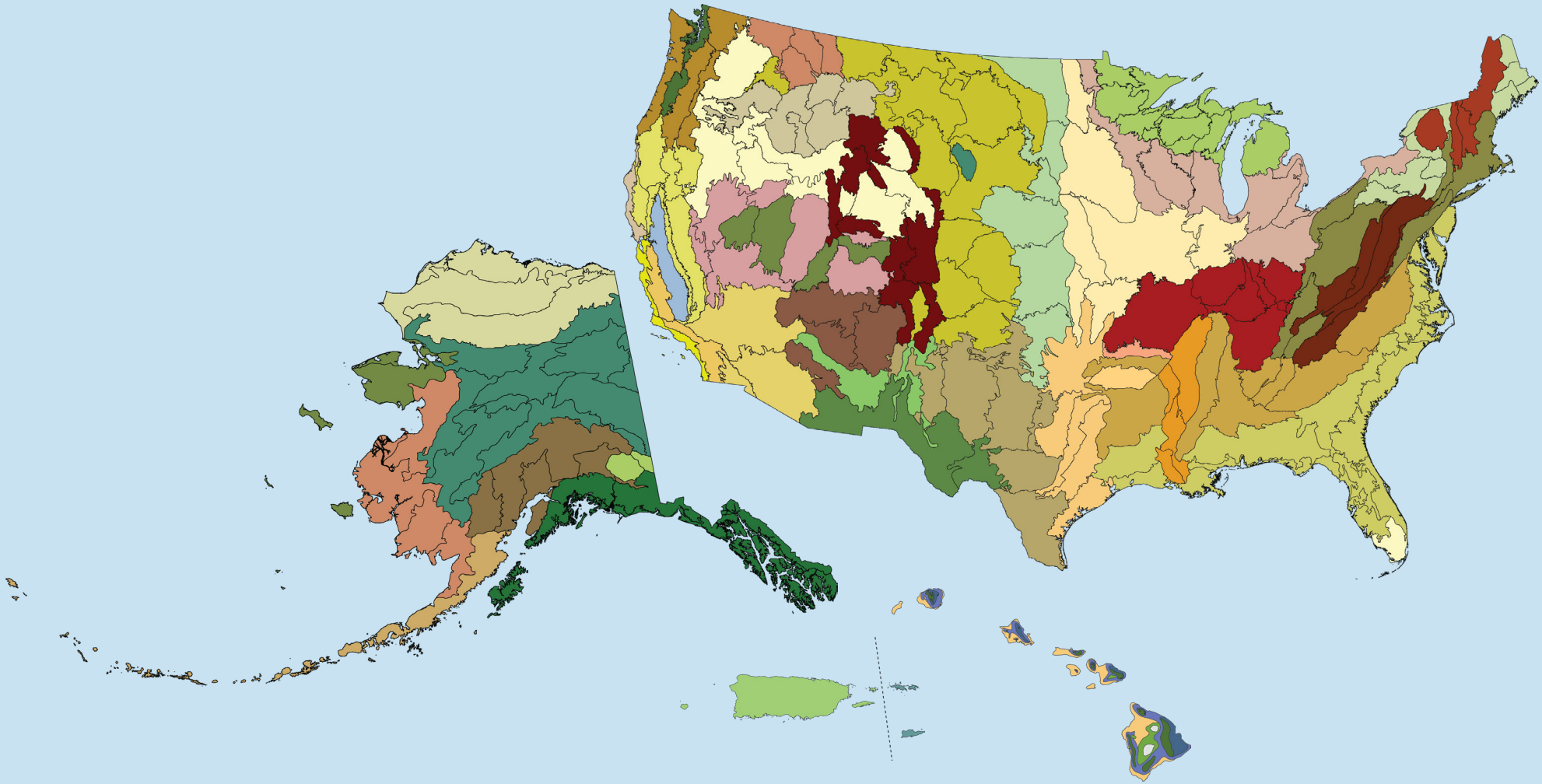

FRONT COVER MAP: Ecoregion provinces and ecoregion sections for the conterminous United States (Cleland et al. 2007) and for Alaska (Spencer et al. 2002), and ecoregions within the islands of Hawaii, along with Puerto Rico and the U.S. Virgin Islands, for which no corresponding ecoregion treatments exist.

BACK COVER MAPS: Tree canopy cover (green) for the conterminous United States, Hawaii, Puerto Rico, and the U.S. Virgin Islands based on data from a cooperative project between the Multi-Resolution Land Characteristics Consortium and the U.S. Department of Agriculture, Forest Service, Geospatial Technology and Applications Center using the 2011 National Land Cover Database (NLCD). Forest and shrubland cover for Alaska derived from the 2011 NLCD.

June 2026
https://doi.org/10.2737/WO-GTR-109a

Forest Health Monitoring: Evaluation Monitoring Project Summaries 2024

EDITORS:

Simone Lim-Hing, Assistant Research Professor, North Carolina State University, Department of Forestry and Environmental Resources, Raleigh, NC 27695

Karun Pandit, Assistant Research Professor, North Carolina State University, Department of Forestry and Environmental Resources, Raleigh, NC 27695

ABSTRACT

Evaluation Monitoring is a component of the Forest Health Monitoring program of the U.S. Department of Agriculture, Forest Service. The overarching goal of Evaluation Monitoring projects is to assess changes in forest health, often at a finer scale than standard monitoring activities. After a project is completed, investigators provide an overview of the scope, methods, and findings. Previous Evaluation Monitoring project summaries are searchable on the Forest Health Monitoring website. This report includes summaries of four recently completed projects: "Using Climate and Remote Sensing Data to Map Current and Future Effects of Balsam Woolly Adelgid in Northern Utah;" "The California Tree Mortality Network: Monitoring Forest Change Following Extreme Drought in the Central and Southern Sierra Nevada, CA;" "Establishing a Monitoring System of Emerald Ash Borer Invasion Impacts on Tribal Black Ash Wetlands;" and "The Impacts of an Exceptional Drought on Forests in Eastern Texas: Disparities in Tree Mortality, Biomass Loss, and Decrease in the Carbon Sink Capacity."

Keywords—Balsam woolly adelgid, bark beetles, California Tree Mortality Network, climate modeling, drought, emerald ash borer, evapotranspiration, hydrological function, tree mortality, wetlands

CONTENTS

CONTENTS

LIST OF FIGURES

LIST OF FIGURES

LIST OF TABLES

EXECUTIVE SUMMARY

The national Forest Health Monitoring (FHM) program of the U.S. Department of Agriculture, Forest Service has an overarching goal to assess the annual changes, trends, and status in forested areas and woodlands. The program operates in partnership with personnel from the Forest Service, State foresters, other State and Federal agencies, and academic groups (e.g., Pandit and Conkling 2024). The program also leverages data from a range of sources, including within and outside of the Forest Service, and develops analytical approaches to address the health and sustainability of forest ecosystems.

Evaluation Monitoring is a component of the FHM program, designed to facilitate projects that assess changes in forest conditions through Detection Monitoring (e.g., using data from aerial or ground surveys; Mangold 2000). This report summarizes four completed Evaluation Monitoring projects funded by the FHM program to address a range of forest health concerns. These projects:

- Quantified and mapped current and potential future effects of balsam woody adelgid (*Adelges piceae*) infestation in northern Utah subalpine fir (*Abies lasiocarpa*) forests. The study combined plot data, remote sensing data, and climate predictors, showing that warmer areas are associated with higher infestation damage severity. Leveraging these relationships provides estimations of how the adelgid can impact factors such as fire fuels and carbon sequestration and enable forest managers to predict and subsequently manage for these effects. Moreover, spatial maps of the balsam wooly adelgid/climate modeling analysis illustrate varying damage severity under current and future climate conditions under different emission scenarios. (ch. 2).
- Reported changes in forest structure after an extreme drought in the Central and Southern Sierra Nevada, CA, using data from plots established by the California Tree Mortality Network—a large-scale, collaborative effort managed by the Forest Service's Pacific Southwest Research Station and Forest Health Protection (Region 5) since 2016. Core variables measured include tree mortality, tree size, invasive plants, pollinators, surface fuels, forest floor composition, and woodborers. Key findings revealed that tree mortality is increasing over time, particularly in lower elevations. Larger diameter ponderosa pine (*Pinus ponderosa*) displayed the highest levels of tree mortality, which is likely due to the western pine beetle (*Dendroctonus brevicomis*) and drought. Tree regeneration was abundantly represented by incense cedar (*Calocedrus decurrens*) and oak (*Quercus* spp.), which may indicate a shift in overstory competition as ponderosa pine mortality increases. (ch. 3).
- Provided a detailed overview of the framework for continuous monitoring of the hydrologic function in Tribal black ash (*Fraxinus nigra*) wetlands prior to emerald ash borer (*Agrilus planipennis*) infestation. The monitoring efforts are a collaboration between the FHM program, the Forest Service's Northern Research Station, and Menominee and Stockbridge-Munsee Community Tribal communities. Two eddy covariance towers have been installed and will be used to obtain high-frequency measurements of evapotranspiration. The study reports the

seasonal trends of evapotranspiration for 2023, establishing a baseline to which to compare future effects of emerald ash borer damage on the wetlands' hydrologic functions (ch. 4).

- Investigated tree mortality, biomass loss, and carbon dynamics attributed to an extreme drought in eastern Texas that occurred in 2011, accounting for spatiotemporal variations on stand characteristics. The yearly average mortality rate during the drought period was 5.89 percent, but estimated effects depended on species (hardwood versus pine), forest type (plantation versus natural forests), and tree size. Pine forests and plantations, for example, had less detrimental responses to the drought. While the drought caused an increase in mortality and decrease in aboveground biomass, metrics partially recovered to the pre-drought levels, suggesting strong resilience. Climate scenario predictions suggest an overall increase in aboveground biomass for the region, but drought scenarios are expected to lower the projected biomass increases by 1.0 to 4.4 percent. Further studies can use this framework and apply additional, interacting disturbances such as hurricanes, fires, and insect outbreaks to predict future effects on forest dynamics (ch. 5).

This report presents some of the latest results from Evaluation Monitoring projects funded by FHM and representing environmental investigations at smaller scales than those at the national scale by FHM and its cooperators. For more information about efforts to determine the status, changes, and trends in indicators of the condition of U.S. forests, please visit the FHM website.

LITERATURE CITED

Mangold, R.D. 2000. Overview of the Forest Health Monitoring program. In: Hansen, M.; Burk, T., eds. Integrated tools for natural resources inventories in the 21st century. Gen. Tech. Rep. NC-212. St. Paul, MN: U.S. Department of Agriculture, Forest Service, North Central Forest Experiment Station: 129–140.

Pandit, K.; Conkling, B.L., eds. 2024. Forest Health Monitoring: national status, trends, and analysis 2023. Gen. Tech. Rep. WO-105. Washington, DC: U.S. Department of Agriculture, Forest Service. 159 p. https://doi.org/10.2737/WO-GTR-105.

CHAPTER 1

Introduction

Simone Lim-Hing and Karun Pandit

The Forest Health Monitoring (FHM) program of the U.S. Department of Agriculture, Forest Service is designed to evaluate trends in forest indicators on an annual basis. The program covers all the Nation's forested lands through a partnership composed of the Forest Service, State foresters, other State and Federal agencies, and academic groups (Pandit and Conkling 2024). The FHM program leverages data from sources both inside and outside the Forest Service and develops analytical approaches for addressing forest health issues that affect forest ecosystems. The program has three major approaches, which are interlinked and provide feedback to each other:

- **Analysis**—Evaluate broad-scale and long-term forest health trends and project future scenarios based on an indicator framework, with technical expertise and inputs from Forest Health Protection and partners.
- **Data integration**—Integrate a variety of data streams to build a rich dataset for forest health analyses.
- **Decision support**—Translate findings from the forest health analysis into meaningful forest health information using different tools and approaches.

Beginning in 2008, the annual FHM report included a section of summaries of completed Evaluation Monitoring projects. These projects, which are funded by the FHM program annually, are intended to address a wide variety of forest health concerns at a smaller scale than the national or multistate regional analyses included in the FHM annual reports. Each summary included an overview of the project and results, citations for projects and other relevant information, and a contact for questions or further information. The summaries showcased the kinds of monitoring projects supported by FHM and included information for readers to pursue specific interests.

In 2023, Evaluation Monitoring project summaries were published separately from the annual FHM report to provide an easier way for readers to locate information on this component of the FHM program, while still documenting and highlighting results of the projects. Current and future Evaluation Monitoring project summaries will continue to be published as separate reports and are searchable on the FHM website reporting page.

Evaluation Monitoring project proposals are selected, reviewed, and submitted through a process established by the FHM Management Team. Each year, this team reviews the proposal guidelines, application instructions, and priorities, culminating in updated proposal instructions and guidelines, new project proposal forms, and progress and final reporting responsibilities being posted on the Forest Health Protection website.[1]

[1] As of 2026, Forest Health Protection special projects are on hiatus indefinitely.

How to cite this chapter:

Lim-Hing, Simone; Pandit, Karun. 2026. Introduction. In: Lim-Hing, Simone; Pandit, Karun, eds. Forest Health Monitoring: Evaluation Monitoring project summaries 2024. Gen. Tech. Rep. WO-109a. Washington, DC: U.S. Department of Agriculture, Forest Service: 3–4. Chapter 1.

This 2024 Evaluation Monitoring project summaries report was produced by FHM researchers at the Eastern Forest Environmental Threat Assessment Center (EFETAC) and project principal investigators across the United States in collaboration with North Carolina State University cooperators in the Forest Health Monitoring Research Group. A unit of the Southern Research Station of the Forest Service, EFETAC was established under the Healthy Forests Restoration Act of 2003 to generate the knowledge and tools needed to anticipate and respond to environmental threats. For more information about the research team and about threats to U.S. forests, please visit the EFETAC website.

LITERATURE CITED

Pandit, K.; Conkling, B.L. eds. 2024. Forest Health Monitoring: national status, trends, and analysis 2023. Gen. Tech. Rep. WO-105. Washington, DC: U.S. Department of Agriculture, Forest Service. 159 p. https://doi.org/10.2737/WO-GTR-105.

CHAPTER 2

Using Climate and Remote Sensing Data to Map Current and Future Effects of Balsam Woolly Adelgid in Northern Utah

Michael J. Campbell and Justin P. Williams

INTRODUCTION

The balsam woolly adelgid (*Adelges piceae*; BWA) is a nonnative, invasive insect that has been infesting and causing damage and mortality to true fir (*Abies* spp.) trees in the United States for more than a century (Hain 1988). In the Western United States, BWA was first identified in the Pacific Northwest around 1930 (Mitchell and Buffam 2001). Since then, it has slowly spread east and south, driving widespread health decline and loss, particularly in subalpine fir (*Abies lasiocarpa*) forests (Livingston et al. 2000). Subalpine fir trees are vulnerable to BWA's effects, though this vulnerability varies regionally and locally according to site conditions (Davis et al. 2022). Only in the last decade has BWA been detected in the State of Utah, having first been identified in the Northern Wasatch Mountains by U.S. Department of Agriculture, Forest Service, Forest Health Protection personnel in 2017 (Davis et al. 2020). Since that time, personnel have put considerable effort toward understanding the spatial distribution of BWA infestation and damaging effects in the State, primarily through aerial and ground surveys. Aerial surveys, although spatially exhaustive, can sometimes lack precision. This is especially true in the case of BWA, whose effects can be subtle, difficult to distinguish from other agents of change, and spatially diffuse (Campbell et al. 2023). Ground surveys are ideally suited for detecting BWA's effects in a robust manner, enabling precise characterization of infestation symptoms (Hrinkevich et al. 2016); however, they are spatially limited to a set of sample points across vast landscapes. Prior to the start of this project, there was a pressing need to develop spatially precise, agent-specific maps of BWA infestation damage severity to establish a baseline for long-term monitoring and inform managers of current damage severities. To address this need, we (the authors of this chapter) conducted a study aimed at mapping the current and potential future effects of BWA infestation in northern Utah. The specific objectives of the study were to:

1. Devise a new approach for quantifying BWA damage severity in the field and collect data on forest structural and damage attributes in plots throughout the Uinta-Wasatch-Cache National Forest to establish a baseline dataset.
2. Compare plot-level damage severity to an array of spatially coincident predictor variables, including satellite image data, topography data, and climate data, to construct a BWA severity predictive model (the focus of Campbell et al. [2023]).
3. Predict how BWA's effects may change over time due to climate and quantify potential losses in subalpine fir biomass over space and time (the focus of Campbell et al. [2024]).

How to cite this chapter:

Campbell, Michael J.; Williams, Justin, P. 2026. Using climate and remote sensing data to map current and future effects of balsam woolly adelgid in northern Utah. In: Lim-Hing, Simone; Pandit, Karun, eds. Forest Health Monitoring: Evaluation Monitoring project summaries 2024. Gen. Tech. Rep. WO-109a. Washington, DC: U.S. Department of Agriculture, Forest Service: 5–13. Chapter 2.

METHODS

Between 2022 and 2023, on 58 plots, we collected BWA infestation and damage severity data to compare and inform the remote sensing and modeling aspects of this study. Plots were strategically distributed throughout the Uinta-Wasatch-Cache National Forest to capture a wide range of infestation damage severity, from completely uninfested to severely impacted. Plots were 15-m fixed-radius circles. We evaluated all subalpine fir trees >5 cm diameter at breast height (d.b.h.) for a series of BWA-specific and other tree health indicators. Here, we provide a brief mention of some key indicators; for a detailed description of the field protocol and approach for quantifying BWA-specific damage severity, see Campbell et al. (2023) and/or Campbell et al. (2024). One of the most important diagnostic indicators of BWA infestation is gouting—abnormal swelling of branch nodes that occurs in response to toxic saliva that BWA inserts into woody tissue during feeding (Balch 1952). Another key indicator of BWA infestation is the presence and abundance of the insects' waxy, woolly coating on the stem of a tree (Retnakaran et al. 1979). In severe crown infestations, BWA can cause crown deformities, including a stunted terminal branch, stunted lateral branches, and a curl in the treetop (Hrinkevich et al. 2016). We aggregated these indicators, along with several others that were not specific to BWA, into a singular, tree-level value, ranging from 0 (no damage) to 1 (maximal damage), that quantified overall tree health. We then proportioned this damage rating into BWA-specific damage versus that from other agents (e.g., bark beetles, fir broom rust, etc.). The BWA-attributed proportional damage values were averaged for all live and recently dead (those with needles still present) subalpine fir trees in each plot, yielding a plot-level measure of BWA infestation damage severity. We did not consider older dead trees (those that no longer retained needles) because damage indicators were difficult or impossible to evaluate and attribute to BWA consistently.

To address our second objective, we compared the 58 plots and their BWA infestation damage severity values to a suite of curated predictor variables specifically designed to capture either signals or potential drivers of severity. With respect to signal predictors, we used a time series of Landsat 8 OLI (Operational Land Imager) and Landsat 9 OLI-2 image data. We used Google Earth Engine (Gorelick et al. 2017) and generated annual growing season (June 1–September 30) cloud-free surface reflectance image composites for each year from 2013 to 2022. We generated a suite of vegetation indices for each year (see table 2 in Campbell et al. [2023]). With these image data, we created two sets of predictors: (1) the spectral conditions (individual band reflectance and indices) at the start of the time series (2013) and (2) a per-pixel temporal linear trend in spectral conditions throughout the entire time series (2013–2022). The former sought to capture pre-infestation vegetation type and structure, whereas the latter sought to capture changes in vegetation condition over time. With respect to potential driver predictors, we derived a series of topographic variables from the U.S. Geological Survey 3D Elevation Program 1 arc-second digital elevation model data (see table 3 in Campbell

et al. [2023]). We also used the digital elevation model to generate a suite of downscaled annual and seasonal climate data using ClimateNA (see table 4 in Campbell et al. [2023], Wang et al. [2016]). With plot-level BWA infestation damage severity as the response variable and these spectral, topographic, and climate datasets as a large set of candidate predictor variables, we used Variable Selection Using Random Forests (VSURF) to distill the predictors down to a parsimonious and meaningful set that could best predict severity (Genuer et al. 2015). We built three random forest models (Breiman 2001) using VSURF-selected predictors: (1) spectral data only (signal model); (2) topographic and climate data only (driver model); and (3) spectral, topographic, and climate data (signal + driver model). All models were assessed using a buffered leave-one-out cross-validation approach (Ploton et al. 2020) and applied to the prediction of BWA damage severity throughout the Uinta-Wasatch-Cache National Forest.

As discussed in the next section, we found that climate data alone were a very strong predictor of BWA infestation damage severity (Campbell et al. 2023). We leveraged the statistical and ecological relationship and conducted a followup study to examine forests' current and future climatic exposure to BWA infestation in northern Utah. Using the same 58-plot database as training and validation, and a similar random forest-based modeling, assessment, and prediction workflow, we built a BWA/climate model that sought to understand climatic drivers of (or at least correlations to) BWA infestation damage severity. ClimateNA, the software for downscaling comparably coarse climate data used in our predictive models, also enables the production of the same downscaled variables for future time periods (Wang et al. 2016). We generated the same set of climatic predictors used in the current (2020) BWA/climate model for four future time periods (2040, 2060, 2080, and 2100) under four climate scenarios, defined as Shared Socioeconomic Pathways (SSP126, SSP245, SSP370, and SSP585; O'Neill et al. 2014). SSP126 represents the most sustainable pathway, with 2.6 W/m^2 of greenhouse gas-driven radiative forcing by 2100. On the opposite extreme, SSP585 represents a very high emissions scenario, with 8.5 W/m^2 of forcing. SSP245 and SSP370 represent more moderate, and perhaps more likely, scenarios. We applied the current model to the prediction of future climatic exposure to BWA damage severity. To yield a tangible measure of the potential impacts of BWA-induced mortality, both present and future, we also modeled subalpine fir aboveground biomass using another random forest modeling framework, trained and validated on the Forest Service's Forest Inventory and Analysis (FIA) data (Bechtold and Patterson 2005). We compared BWA damage severity maps to subalpine fir biomass maps to yield a per-pixel estimate of potential biomass loss, which can serve as a proxy for fire fuels, carbon sequestration, and a range of ecosystem services. We then compiled the results of this analysis into a public-facing dashboard, enabling all interested parties to better understand the spatial dimensions of the BWA and climate relationship and potential effects in a changing climate.

RESULTS

The severities in our plot database ranged from 0.00 to 0.49, with the former representing areas where BWA is either not present or has had no detectable effects on forest health and the latter representing a relatively severe infestation. The scale of our severity rating system theoretically could be as high as 1.00; however, this would require that all subalpine fir trees were dead in a plot, all of the BWA indicator metrics were rated as maximally severe for each tree, and there was no evidence of any other agents—an unlikely combination even in extreme cases. In all, we measured 2,409 trees in the 58 plots, 62 percent of which had at least some indication of BWA infestation.

Of the three models that sought to map current BWA infestation damage severity, the spectral-only model (which aimed to quantify the signal of severity) performed the worst according to both variances explained (R^2) and predictive errors (root mean square error [RMSE]). R^2 between predictions and observations ranged from 0.391 to 0.541, depending on the cross-validation buffer distance (fig. 2.1). The selected predictors featured a mix of pre-infestation and change metrics, the former of which captured regional variation in subalpine fir forest structure and composition and the latter of which pointed towards decreased photosynthetically active radiation absorption and decreased moisture in higher severity pots. The terrain and climate-only model (which aimed to quantify the potential drivers of severity) performed better, with R^2 ranging from 0.737 to 0.761. This model yielded a very parsimonious set of four climate variables (no topographic variables), all of which pointed toward a positive relationship between seasonal and annual temperatures and damage severity. The combined model, which featured spectral, topographic, and climate variables as candidate predictors and sought to quantify both signal and potential drivers of severity, performed the best (R^2 ranged from 0.827 to 0.852). The mapped results of the combined model yielded the best available depiction of current BWA infestation damage severity in the Uinta-Wasatch-Cache National Forest, which pointed toward localized hotspots of severity in the Central and Northern Wasatch Mountains and comparably limited severity in the Uinta Mountains, primarily contained to the westernmost and lowest elevation flanks.

The BWA/climate modeling analysis yielded novel insight into the spatial dimensions of current and potential future effects of BWA in northern Utah. The model had four predictor variables (listed in order of decreasing importance): (1) minimum spring temperature, (2) number of annual frost-free days, (3) degree days below zero in autumn, and (4) number of frost-free days in spring. All pointed toward the same underlying relationship—that warmer areas (more frost-free days, higher minimum temperatures, lower degree days below zero) correspond to higher BWA infestation damage severity. Projecting this model throughout the 21st century revealed that, under lower emissions scenarios (SSP126, SSP245), BWA's effects remain largely contained to the lower elevation, warmer Wasatch Mountains, with the highest elevation areas remaining somewhat robust against the insect.

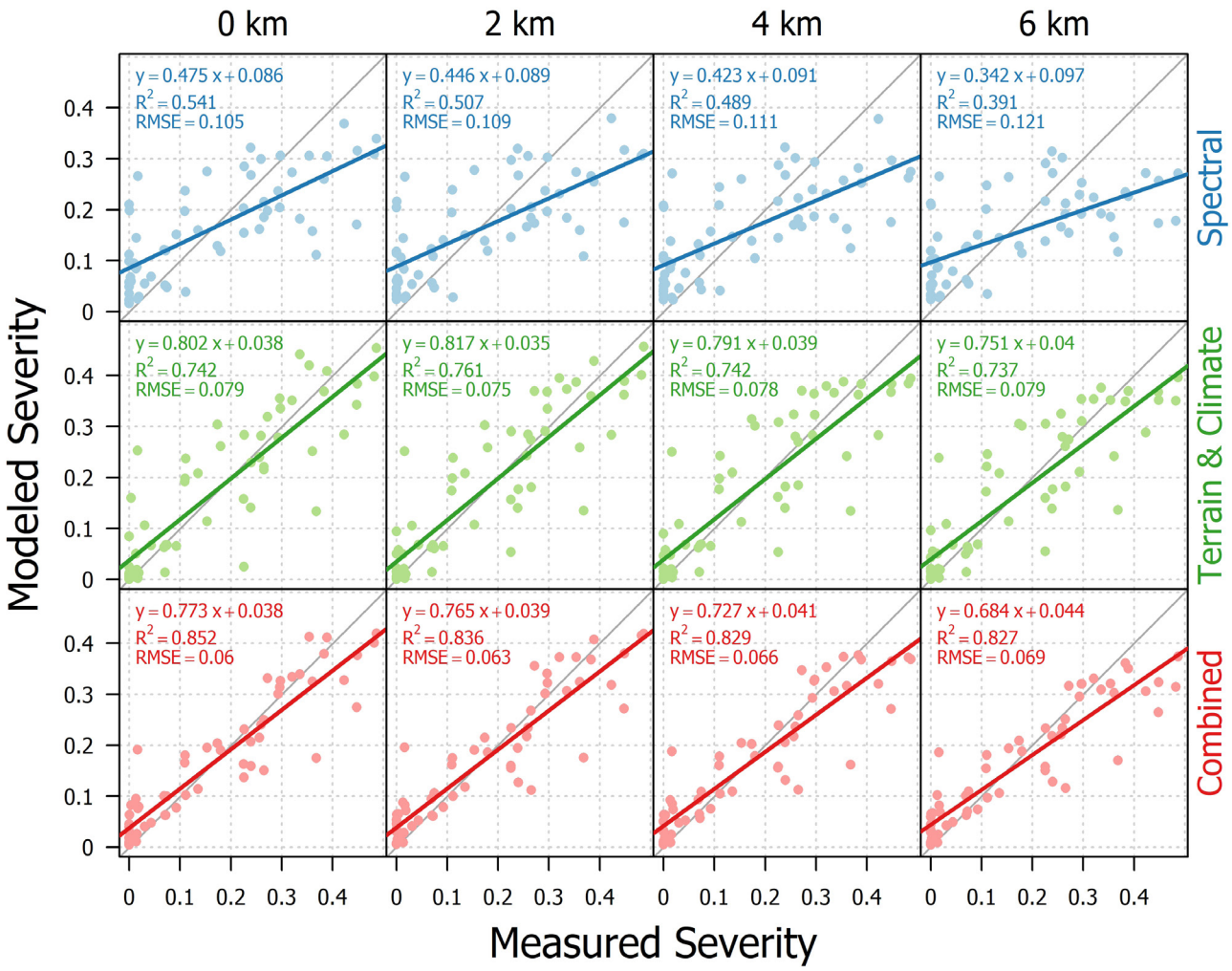

Figure 2.1—Results from the current balsam woolly adelgid infestation damage severity modeling exercise, comparing predictions and observations from three different model types (rows) made using four different buffered leave-one-out cross validations (columns), with associated performance metrics. Source: Campbell et al. (2023).

Under higher emissions scenarios (SSP370, SSP585), in addition to high damage severity throughout the entirety of the Wasatch, BWA may very well cause widespread damage in the higher and cooler Uinta Mountains as well. The biomass predictive model explained nearly half of the variance in field-measured biomass (R^2 = 0.448) and made predictions with errors <7 Mg/ha (RMSE = 6.177 Mg/ha). We applied this model to map biomass throughout the study area, of which we compared on a per-pixel basis to the various BWA/climate projections, yielding joint severity-biomass estimates. In 2020, 59 percent of all mapped subalpine fir in our study area had very low to no damage severity. By 2100, this shrinks to 48 percent under SSP126, 21 percent under SSP245, 1 percent under SSP370, and 0 percent under SSP585. Under the SSP245 scenario, 1.9 Tg of biomass (~50 percent of which is carbon) will be exposed to high BWA infestation damage severity by 2100 in our study area. Figure 2.2 conveys the joint severity-biomass estimates under the moderate SSP245 scenario averaged out for the middle of the 21st century. These results suggest that the Northern Wasatch in particular is poised to see significant increases in BWA-induced damage.

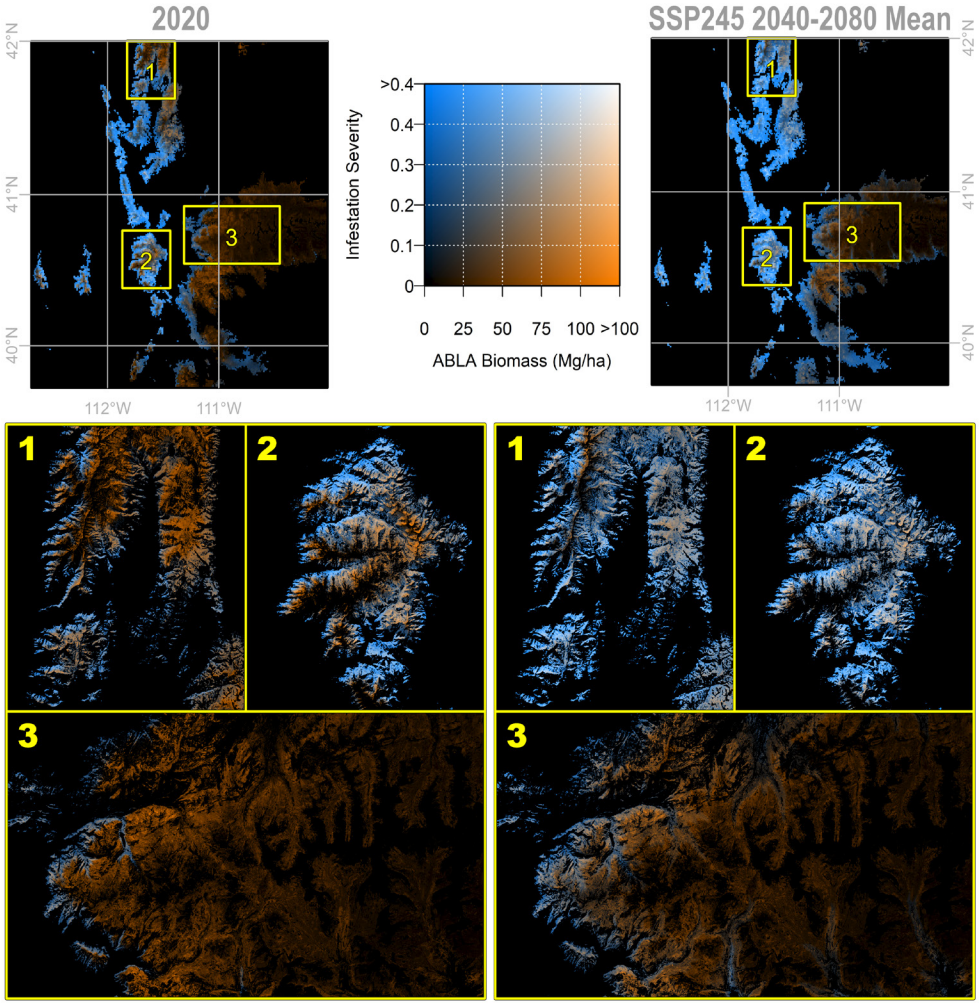

Figure 2.2—Results from the balsam woolly adelgid (BWA)/climate modeling analysis, featuring a comparison between 2020 climatic exposure to BWA damage severity and that from a 2040–2080 mean under the SSP245 climate scenario in subalpine fir (Abies lasiocarpa) *forests of northern Utah. The map depicts both the Wasatch and Uinta Mountain ranges. Pixel values are colors according to the bivariate color palette featured in the top-center of the figure that quantifies both subalpine fir (ABLA) biomass and infestation damage severity. Three focal areas are highlighted to illustrate areas that feature different levels of projected future BWA effects: (1) the Bear River Range in the Northern Wasatch Mountains, (2) the Central Wasatch Mountains east of the Salt Lake Valley, and (3) the Western Uinta Mountains. Source: Campbell et al. (2024)*

DISCUSSION

Evaluating BWA impacts is challenging even at a distance of a few meters, let alone from an aircraft or a satellite. Implicit in our second major objective was a goal to understand the degree to which a satellite image time series could be used to quantify and map BWA's damaging effects on subalpine fir trees in northern Utah. Although Landsat data captured approximately half of the variance in ground-observed severity, the half that was left unexplained is likely attributable to a few factors. These include:

- **Spatial diffuseness of BWA damage severity**—BWA damage is somewhat unlike that of other forest pests because trees in relatively close proximity can feature significantly different degrees of apparent effects. Given the moderate spatial resolution of Landsat pixels (30 m), this means that a lot of spectral mixing from healthy and unhealthy trees within a single pixel can compromise the ability to detect change.
- **Temporal longevity of BWA-induced tree health decline**—BWA can take years to kill a tree (Davis et al. 2022). Satellite imagery is well suited to the task of mapping temporally discrete disturbance events (e.g., fire and timber harvest), but drawn-out spectral changes are more difficult to discern.
- **Confusion with other agents of change**—Changes in spectral response over time, such as a decrease in greenness, can be caused by any number of agents. Given that BWA almost never acts alone to kill a tree and that other agents are acting to impact both subalpine fir and its cohabitant species throughout northern Utah, the Landsat data alone were unable to attribute spectral changes specifically to BWA.

The BWA and climate relationship that emerged in our second objective and was exploited in our third objective was impressively strong. Using four climate variables, nearly 80 percent of variance in observed damage severity was explained by our BWA/climate model. We cannot precisely state whether this has to do with BWA's preference for warmer areas or subalpine fir's increased susceptibility in these areas, but the answer likely lies in some combination of these two factors. White fir (*Abies concolor*) trees tend to grow in lower elevation, warmer environments than subalpine fir and are also a host species for BWA but have shown little evidence of widespread negative damage due to the insect. This would point more toward subalpine fir's vulnerability in warmer areas rather than BWA's preference for them, but more research is needed to better understand the potential landscape drivers of subalpine fir's vulnerability to BWA. Our maps will provide a useful starting point for such entomological investigations. If the BWA and climate relationship is sufficiently robust and the insect has sufficient opportunity to spread throughout northern Utah, a warming climate is anticipated to promote both expanded and increased damage severity as greater proportions of subalpine fir forests become exposed to higher annual and seasonal temperatures.

CONCLUSIONS

Having only recently spread into Utah, BWA's effects in the State have been increasing rapidly. Prior to the start of our work, knowledge of the statewide extent and severity of BWA infestation was limited to ground and aerial surveys. Here, we described an analytical approach for accurately quantifying and mapping BWA's effects and found a strong predictive relationship between annual and seasonal climatic temperature and severity. This relationship provided fertile ground for the spatially explicit estimation of potential future BWA effects on Utah's subalpine fir forests. Tying damage severity to biomass resulted in a quantifiable understanding of BWA's potential effects on fire fuels and ecosystem services as well as enabled forest managers to proactively mitigate these effects through targeted silvicultural strategies.

Several avenues for potential future research would enhance the impact of this study. The first is to replicate the analysis approach for mapping current BWA infestation using remotely sensed and climate data in future years, which will allow for retrospective evaluations of the expansion or enhancement of BWA's effects over time. The second is to expand the spatial scope of either of our modeling approaches to include broader regional areas where BWA has infested. This will allow for a more consistent and exhaustive monitoring procedure than can be done with ground and aerial surveys alone and may provide valuable insight into other parts of the Intermountain West where the climate may promote BWA's damaging effects.

For more information, contact: Michael Campbell, mickey.campbell@ess.utah.edu

LITERATURE CITED

Balch, R.E. 1952. Studies on the balsam woolly aphid (*Adelges piceae* Ratz.) and its effects on balsam fir, *Abies balsamea* (L.) Mill. Ottawa, Canada: Department of Agriculture. 76 p.

Bechtold, W.A.; Patterson, P.L., eds. 2005. The enhanced Forest Inventory and Analysis program—national sampling design and estimation procedures. Gen. Tech. Rep. SRS-80. Asheville, NC: U.S. Department of Agriculture, Forest Service, Southern Research Station. 85 p.

Breiman, L. 2001. Random forests. Machine Learning. 45: 5–32. https://doi.org/10.1023/A:1010933404324.

Campbell, M.J.; Williams, J.P.; Berryman, E.M. 2023. Using remote sensing and climate data to map the extent and severity of balsam woolly adelgid infestation in northern Utah, USA. Forests. 14: 1357. https://doi.org/10.3390/f14071357.

Campbell, M.J.; Williams, J.P.; Berryman, E.M.; Anderegg, W.R.L. 2024. Quantifying current and potential future impacts of balsam woolly adelgid infestation on forest biomass. Forest Ecology and Management. 560: 121852. https://doi.org/10.1016/j.foreco.2024.121852.

Davis, G.; Lowrey, L.; Eckberg, T. [et al.]. 2020. Notes on balsam woolly adelgid, *Adelges piceae* (Ratzeburg, 1844) (Hemiptera: Adelgidae), range expansion in Idaho, Montana and Utah. The Pan-Pacific Entomologist. 96(3): 129–133. https://doi.org/10.3956/2020-96.3.129.

Davis, G.; Lowrey, L.; Eckberg, T. [et al.]. 2022. Characterizing balsam woolly adelgid infestations and associated tree mortality in Idaho. Journal of Forestry. 120(4): 361–378. https://doi.org/10.1093/jofore/fvac007.

Genuer, R.; Poggi, J.-M.; Tuleau-Malot, C. 2015. VSURF: an R package for variable selection using random forests. The R Journal. 7: 19–33. https://doi.org/10.32614/RJ-2015-018.

Gorelick, N.; Hancher, M.; Dixon, M. [et al.]. 2017. Google Earth Engine: planetary-scale geospatial analysis for everyone. Remote Sensing of Environment. 202: 18–27. https://doi.org/10.1016/j.rse.2017.06.031.

Hain, F.P. 1988. The balsam woolly adelgid in North America. In: Berryman, A.A., ed. Dynamics of forest insect populations: patterns, causes, implications, population ecology. Boston, MA: Springer: 87–109. https://doi.org/10.1007/978-1-4899-0789-9_5.

Hrinkevich, K.H.; Progar, R.A.; Shaw, D.C. 2016. A severity rating system for evaluating stand-level balsam woolly adelgid (Hemiptera: Adelgidae) damage in two *Abies* species in Western North America. Forest Science. 62(2): 181–189. https://doi.org/10.5849/forsci.15-025.

Livingston, R.L.; Dewey, J.E.; Beckman, D.P.; Stipe, L.E. 2000. Distribution of the balsam woolly adelgid in Idaho. Western Journal of Applied Forestry. 15(4): 227–231. https://doi.org/10.1093/wjaf/15.4.227.

Mitchell, R.G.; Buffam, P.E. 2001. Patterns of long-term balsam woolly adelgid infestations and effects in Oregon and Washington. Western Journal of Applied Forestry. 16(3): 121–126. https://doi.org/10.1093/wjaf/16.3.121.

O'Neill, B.C.; Kriegler, E.; Riahi, K. [et al.]. 2014. A new scenario framework for climate change research: the concept of shared socioeconomic pathways. Climatic Change. 122: 387–400. https://doi.org/10.1007/s10584-013-0905-2.

Ploton, P.; Mortier, F.; Réjou-Méchain, M. [et al.]. 2020. Spatial validation reveals poor predictive performance of large-scale ecological mapping models. Nature Communications. 11: 4540. https://doi.org/10.1038/s41467-020-18321-y.

Retnakaran, A.; Ennis, T.; Jobin, L.; Granett, J. 1979. Scanning electron microscopic study of wax distribution on the balsam woolly aphid, *Adelges piceae* (Homoptera: Adelgidae). The Canadian Entomologist. 111(1): 67–72. https://doi.org/10.4039/Ent11167-1.

Wang, T.; Hamann, A.; Spittlehouse, D.; Carroll, C. 2016. Locally downscaled and spatially customizable climate data for historical and future periods for North America. PLoS ONE. 11(6): e0156720. https://doi.org/10.1371/journal.pone.0156720.

CHAPTER 3

The California Tree Mortality Network: Monitoring Forest Change Following Extreme Drought in the Central and Southern Sierra Nevada, CA

Christopher J. Fettig, Leif A. Mortenson, Beverly M. Bulaon, Crystal S. Homicz, Jackson P. Audley, and Justin B. Runyon

How to cite this chapter:

Fettig, Christopher J.; Mortenson, Leif A.; Bulaon, Beverly M.; Homicz, Crystal S.; Audley, Jackson P.; Runyon, Justin B. 2026. The California Tree Mortality Network: monitoring forest change following extreme drought in the Central and Southern Sierra Nevada, CA. In: Lim-Hing, Simone; Pandit, Karun, eds. Forest Health Monitoring: Evaluation Monitoring project summaries 2024. Gen. Tech. Rep. WO-109a. Washington, DC: U.S. Department of Agriculture, Forest Service: 15–28. Chapter 3.

INTRODUCTION

Climates in California range widely, from desert to subarctic, but much of California experiences a Mediterranean-type climate characterized by seasonal dry and wet periods. For example, California receives most (>95 percent) precipitation in the form of rain and high-elevation (>1829 m) snow between October and May (Swain et al. 2016). Both seasonal and annual droughts are common in California (Cook et al. 2007). In forests, droughts reduce tree growth, increase wildfire hazards, and incite bark beetle outbreaks and extensive tree mortality (fig. 3.1), all of which in turn affect biogeochemical cycling and hydrologic processes. In rangelands, droughts reduce plant and forage productivity, alter nutrient cycling, increase wildfire hazards, and increase susceptibility to invasions by nonnative plants (Fettig et al. 2019b). In California, 21st century droughts have been characterized by large precipitation deficits and high temperatures. This is exemplified by the 2012–2015 drought (Luo et al. 2017) during which winter 2014–2015 was the warmest on record and the year 2014 was the driest (based on Palmer Drought Severity Index, which uses temperature and precipitation to estimate relative dryness). While the 2012–2015 drought was widespread throughout California, conditions were most severe in parts of the Central and Southern Sierra Nevada.

The U.S. Department of Agriculture, Forest Service's national Insect and Disease Survey reported extensive levels of tree mortality in California in 2015. Mortality was concentrated in the Central and Southern Sierra Nevada. The survey estimated 29 million and 62 million trees died in 2015 and 2016, respectively, due largely to drought and outbreaks of native bark beetles. About 237 million trees have died since 2010. Though approximately 200 species of bark beetles are native to California, only a few species cause extensive tree mortality (Fettig 2016). Drought often incites bark beetle outbreaks, including those of several species endemic to the Central and Southern Sierra Nevada: engraver beetles (*Ips* spp.), fir engraver (*Scolytus ventralis*), Jeffrey pine beetle (*Dendroctonus jeffreyi*), mountain pine beetle (*D. ponderosae*), and western pine beetle (*D. brevicomis*). Kolb et al. (2016) reported a nonlinear relationship between drought intensity and bark beetle performance, where moderate drought reduces bark beetle performance and subsequent tree mortality and severe drought increases bark beetle performance and subsequent tree mortality. Drought reduces carbon assimilation, water transport, and synthesis and mobilization of oleoresin. Conifers mobilize oleoresin following wounding, which is an important defense against bark beetles as pioneering beetles are often encapsulated and killed in oleoresin (Franceschi et al. 2005).

Figure 3.1—Tree mortality on the Sequoia National Forest, CA, 2017. Most of the faded trees were colonized and killed by bark beetles the previous year following a period of extreme and exceptional drought. Forest Service photo by C.J. Fettig.

The California Tree Mortality Network (CTMN) exists to enhance understanding of the biophysical drivers, effects, and consequences of tree death in seasonally dry forests in California. Resultant information is used to better inform management responses, including adaptation, mitigation, restoration, and recovery. More recent efforts integrate study and understanding of hydroclimatic extremes and simulate forest recovery under different climate regimes. The CTMN is a large-scale, long-term, collaborative effort managed by the Pacific Southwest Research Station and Forest Health Protection (Region 5). A complete description of CTMN-related research is beyond the scope of this summary. This chapter describes the structure of the CTMN and highlights select research findings.

METHODS

The CTMN comprises 180 fixed-radius plots (11.3 m [0.041 ha] each), which were established on the Eldorado, Stanislaus, Sierra, and Sequoia National Forests, CA, in 2016–2017 (fig. 3.2). Fifteen plots (three groups of five plots) are distributed in each of three elevation bands on each national forest: 914–1219 m, 1219–1524 m, and 1524–1829 m on the Eldorado, Stanislaus, and Sierra, and 1219–1524 m, 1524–1829 m, and 1829–2134 m on the Sequoia. The Sequoia National Forest is the most southerly in the CTMN (fig. 3.2), and ponderosa pine (*Pinus ponderosa*) seldom grows there below ~1524 m elevation. This explains the increase in elevation bands on the Sequoia National Forest compared to the Eldorado, Stanislaus, and Sierra National Forests. At establishment, plots were required to be ≥35 percent ponderosa pine by basal area, to contain ≥10 percent ponderosa pine mortality in the last 2 years, and to be unburned in the last decade. We (the authors of this chapter) selected these criteria as our primary objective was to monitor changes in forest conditions resulting from tree mortality attributed to drought and bark beetle outbreaks, which were most severe in ponderosa pine. We randomly selected plots meeting these criteria and separated plots by ≥100 m within groups. Groups within elevation bands were separated by >1.6 km.

On each plot, we numbered and georeferenced trees ≥6.35 cm diameter at breast height (d.b.h.; 1.37 m in height) and recorded the species, d.b.h., height, height to the base of the live crown, condition (live or dead, based on the presence or absence of crown fade), cause of death (if applicable), and year of death (if applicable). For trees that died prior to plot establishment, we estimated year of death based on the color of faded needles in the crown and degree of needle retention (1 year prior = >90 percent retention of yellow and/or red needles; 2 years prior = ≥50 to 90 percent retention of red needles; ≥3 years prior = <50 percent retention of red and/or gray needles). Trees that died ≥3 years prior to plot establishment were ignored.

For dead trees (determined by crown fade), we used a hatchet to remove a ~625-cm^2 section of bark at ~2 m in height on the north and south aspects to determine if bark beetle galleries were present. The shape, distribution, and orientation of galleries were used to distinguish among bark beetle species. In some cases, deceased bark beetle adults were present beneath the bark, which supplemented identifications based on

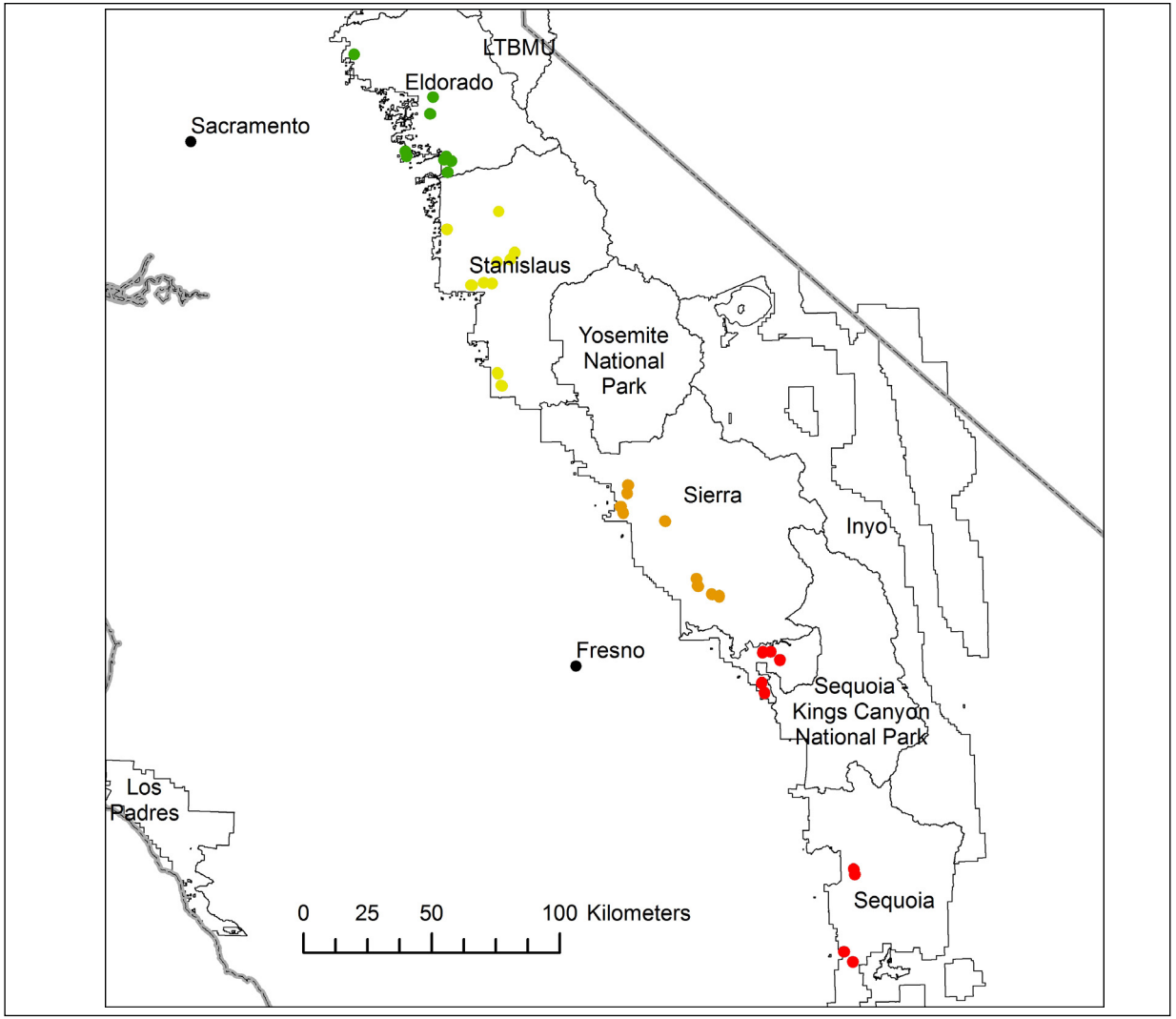

Figure 3.2—The California Tree Mortality Network consists of 180 fixed-radius plots (11.3 m [0.041 ha] each) on 4 national forests within 3 elevation bands. The locations of plots are depicted with green points (Eldorado National Forest), yellow points (Stanislaus National Forest), orange points (Sierra National Forest), and red points (Sequoia National Forest). Several points overlap due to spatial scale (each national forest contains 45 plots). Thirty-five plots were lost to wildfires in recent years.

gallery formation. We attributed tree mortality to colonization by western pine beetle, mountain pine beetle, California fivespined ips (*I. paraconfusus*), pine engraver (*I. pini*), fir engraver, and cedar bark beetles (*Phloeosinus* spp.) only when parental and brood galleries were observed in or beneath the sections of bark removed, despite the presence of other potential diagnostic characteristics (e.g., pitch tubes higher on the tree bole). As such, our estimates of levels of tree mortality attributed to bark beetles are conservative. Suppression was assigned as the cause of death when evidence of other contributing factors (e.g., bark beetles, pathogens, and mechanical damage) were absent and the tree received little or no direct sunlight from above or on the sides of the crown. In rare cases, we could not identify a contributing factor and the cause of death was recorded as unknown.

To measure ground and surface fuels, we established three Brown's transects (Brown 1974) at 0°, 120°, and 240° from the center of each CTMN plot. A 0.004-ha (3.6-m radius) subplot was established at the center of each plot to estimate seedling (≤0.3 m tall) and sapling (>0.3 m tall to <6.35 cm d.b.h.) abundance by species, as well as ground and shrub cover. On each plot, we conducted a complete census for the presence of invasive plants listed as "currently causing damage in California" (California Invasive Plant Council 2024). We sampled forest pollinators on 24 CTMN plots for a 24-hour period on 5 occasions (every other week) each year that pollinator sampling occurred (table 3.1), employing bee cups and blue vane traps using standard protocols. Pollinator sampling was staggered temporally by elevation band to account for differences in temperature among bands that influence pollinator activity (Pyke et al. 2011). In 2022 and 2023, we sampled woodborer and other beetle communities on a subset of CTMN plots representing three disturbance classes: (1) less disturbed (2022, <30 percent tree mortality)/undisturbed (2023, <10 percent tree mortality), (2) high tree mortality and low snag fall (≥50 percent tree mortality, ≤50 percent snag fall), and (3) high tree mortality and high snag fall (≥50 percent tree mortality, >60 percent snag fall). Panel traps with high-release ethanol lures were deployed using standard protocols.

Tree mortality and snag fall occurrences have been recorded each year since the establishment of the CTMN. Other core variables are recorded less frequently (table 3.1).

Table 3.1—Core variables measured on the California Tree Mortality Network, 2016–2025

Variable	2016	2017	2018	2019	2020	2021	2022	2023	2024	2025
Tree mortality	X[1]	X	X	X	X	X	X	X	X	X
Snag fall occurrences	X[1]	X	X	X	X	X	X	X	X	X
Tree d.b.h. (including ingrowth)	X[1]	X[2]	—	—	X[1]	X[2]	—	—	X[1]	X[2]
Tree height	—	X	—	—	—	X	—	—	—	X
Height to base of live crown	—	X	—	—	—	X	—	—	—	X
Ladder fuels	—	X	—	—	—	X	—	—	—	X
Live crown cover	—	X	—	—	—	—	X	—	—	X
Tree regeneration	X[1]	X[2]	—	—	X[1]	X[2]	—	—	X[1]	X[2]
Forest floor composition	—	X	—	—	—	—	X	—	—	X
Invasive plants	—	X	—	—	—	—	X	—	—	X
Shrub species cover (% and height)	—	X	—	—	—	—	X	—	—	X
Surface fuels	—	X	—	X	—	X	—	X	—	—
Litter and duff	—	X	—	X	—	X	—	X	—	—
Pollinators	—	X[3]	—	—	—	—	X[3]	—	—	X[3]
Woodborers	—	—	—	—	—	—	X[3]	X[3]	—	—

d.b.h. = diameter at breast height.
X = measured on all plots.
X[1] = measured on plots established in 2016.
X[2] = measured on plots established in 2017.
X[3] = measured on a select subset of plots.
— = not measured.

RESULTS AND DISCUSSION

Fettig et al. (2019a) described causal agents and rates of tree mortality, as well as short-term effects on forest structure and composition. About 48.9 percent of trees died between 2014 and 2017 (fig. 3.3A). Tree mortality ranged from 46.1 ± 3.3 percent (mean ± standard error of the mean [SEM], all cases) on the Eldorado National Forest to 58.7 ± 3.7 percent on the Sierra National Forest. Significantly higher levels of tree mortality occurred in the low-elevation band (60.4 ± 3.0 percent) compared to the high-elevation band (46.1 ± 2.9 percent). Ponderosa pine exhibited the highest levels of tree mortality (89.6 percent), with 39.4 percent of CTMN plots losing all ponderosa pines. Mortality of ponderosa pine was highest at the lowest elevations, concentrated in larger diameter trees (fig. 3.3B), and attributed primarily to western pine beetle. No mortality occurred in ponderosa pines ≤10.0 cm d.b.h. Sugar pine (*P. lambertiana*) exhibited the second highest levels of tree mortality (48.1 percent). Mortality of sugar pine was concentrated in the mid-diameter classes and attributed primarily to mountain pine beetle. White fir (*Abies concolor*) and incense cedar (*Calocedrus decurrens*) exhibited 26.3 and 23.2 percent mortality, respectively. Only one oak (*Quercus* spp.) tree died between 2014 and 2017. Since 2017, limited tree mortality has occurred on the CTMN with the exception of white fir (2017–2019), which was attributed to the direct effects of wildfires (2020–2021). Thirty-five CTMN plots were impacted by wildfires in 2020 (Creek Fire, 5 plots) and 2021 (Caldor Fire, 10 plots; French Fire, 5 plots; KNP Complex Fire, 5 plots; Windy Fire, 10 plots). A smaller pulse in tree mortality since 2017 resulted from ponderosa pine and sugar pine snags falling, crushing, and killing remnant trees (fig. 3.4), including the previously mentioned oak. The fall rate of beetle-killed trees on the CTMN is much faster (e.g., more than two times faster) than reported in most other studies in the Western United States (e.g., the half-life of lodgepole pine [*P. contorta*] killed by mountain pine beetle in the Intermountain West is ~16 years since death; Audley et al. 2021). A peer-reviewed publication on snag demography is in preparation.

Tree regeneration on the CTMN is dominated by incense cedar and oak species, which represents a potential shift in overstory composition from forests that were mostly dominated by ponderosa pine prior to the 2012–2015 drought. Ponderosa pine is regenerating naturally on many CTMN sites but at lower (mean) abundances than incense cedar, white fir, or California black oak (*Q. kelloggii*). Total seedlings and saplings increased from 1,620 ± 195/ha and 1,903 ± 252/ha at CTMN establishment to 2,522 ± 68/ha and 2,869 ± 346/ha in 2020–2021, respectively. Regeneration and recruitment have been highly variable (high standard error) across the CTMN, necessitating longer term observations to project changes in overstory composition with much certainty.

Mountain misery or bearclover (*Chamaebatia foliolosa*), whiteleaf manzanita (*Arctostaphylos viscida*), and greenleaf manzanita (*A. patula*) are the most abundant shrubs on the CTMN. Competition by these species has reduced tree seedling survival and inhibited tree seedling growth (e.g., Tappeiner and Radosevich 1982, White and Newton 1989), especially for ponderosa pine. In general, shrubs capture and

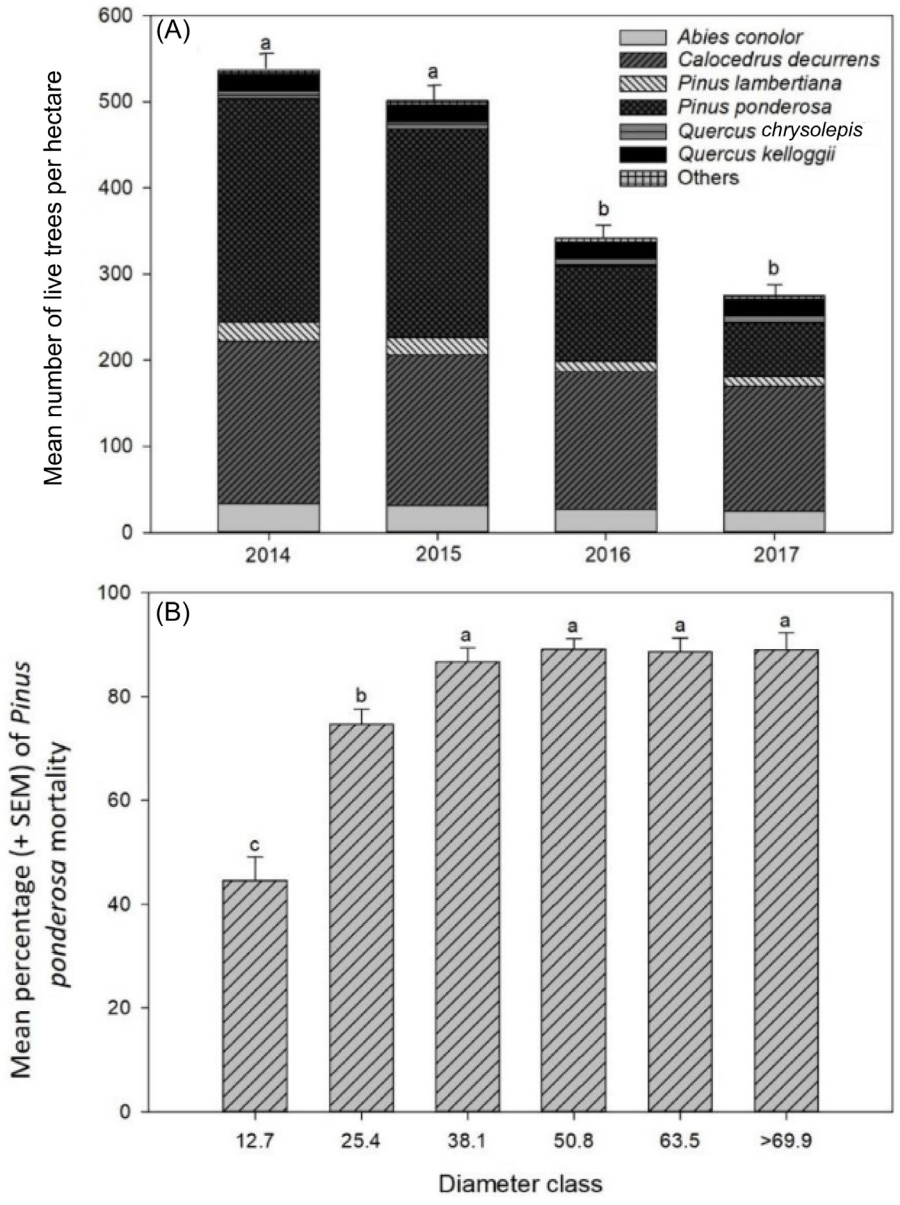

Figure 3.3 —(A) Mean number of live trees per hectare and (B) mean percentage of ponderosa pine (Pinus ponderosa) *mortality by diameter class (midpoint of 12.7-cm diameter classes, except for largest) on the Eldorado, Stanislaus, Sierra, and Sequoia National Forests, CA, 2014–2017. Means (+ SEM) followed by the same letter within each figure are not significantly different (p >0.05).*

Figure 3.4—Snag fall on a California Tree Mortality Network plot on the Stanislaus National Forest, 2019. The large-diameter snags are ponderosa pine killed by western pine beetle. Forest Service photo by L.A. Mortenson.

uptake soil moisture at much lower concentrations than trees, buffering shrubs from drought stress (Hurteau and North 2008). Limited mortality of shrubs has occurred and mountain misery remains the dominant shrub species. The mean height of mountain misery, whiteleaf manzanita, and greenleaf manzanita remains unchanged.

At establishment, ~22 percent of CTMN plots contained one or more invasive plant species, including cheatgrass (*Bromus tectorum*), ripgut brome (*B. diandrus*), bull thistle (*Cirsium vulgare*), and yellow star-thistle (*Centaurea solstitialis*). Since plot establishment, the presence of cheatgrass has increased from ~9 percent of plots to ~25 percent of plots. Cheatgrass is a notable invasive weed that is enhanced by elevated CO2 and temperature (Zelikova et al. 2013), making this species more competitive in these conditions. Other invasive plant species have decreased in occurrence on the CTMN or disappeared.

Vilanova et al. (2023) characterized ground (duff) and surface fuels shortly after the drought in 2016–2018. Their analyses used CTMN data in addition to other data available from a similar network of plots maintained by the University of California. Overall, they reported high fuel biomasses for most sites (mean = 138.2 Mg/ha), with values up to five times higher than estimates for presettlement conditions for mixed-conifer forests (e.g., mean = 26.9 Mg/ha; Stephens et al. 2007). They identified four major groups of forest overstory structure with some distinct fuel characteristics. These ranged from a cluster of ponderosa pine-dominated plots with the highest density of snags (trees colonized and killed by western pine beetle), lowest live tree basal area, and lowest total ground fuel and surface fuel biomass (mean = 90.1 Mg/ha) to a group of giant sequoia (*Sequoiadendron giganteum*)-dominated plots with the highest live tree basal area and highest total fuel biomass (mean = 547.6 Mg/ha). Ground and surface fuels are measured regularly across the CTMN (table 3.1) and have increased substantially in some, but not all, fuel classes. A peer-reviewed publication on changes in fuel loads based on measurements in 2019, 2021, and 2023 is in the final stages of preparation.

Koontz et al. (2021) conducted aerial surveys using drones over 160 CTMN plots along a climatic water deficit (the amount of water by which potential evapotranspiration exceeds actual evapotranspiration) gradient spanning 350 km of latitude and 1000 m of elevation. Over 450,000 trees were mapped, measured, and classified. Aerial estimates were validated with data from CTMN plots. Mortality of ponderosa pine (the only host of western pine beetle in these forests) increased with size, proportion, and density, as well as climatic water deficit. Larger trees amplified host mortality rates on hot/dry sites. Fettig et al. (2019a) reported tree mortality was positively correlated with initial live tree density and slope on the CTMN. A time lag was observed between the occurrence of drought (2012–2015) and the majority of tree mortality (2016; fig. 3.3A).

Using a novel model of bark beetle biology and host tree interactions, Robbins et al. (2022) assessed how contemporary warming affected western pine beetle populations during the 2012–2015 drought. They reported that warming increased the development rate of western pine beetles and decreased their overwintering mortality rate, leading to increased population growth. During the drought period, the number of western pine beetles in flight was projected to be 35.1 percent higher at the initiation of the drought and to remain elevated (37.4 to 45.4 percent) during the drought, compared to historic simulations. Overall, Robbins et al. (2022) projected that ~30 percent of the increase in ponderosa pine mortality during the drought was attributed to the direct effects of warming on western pine beetle populations. The remaining 70 percent was attributed to the indirect effects of warming and drought on host susceptibility to western pine beetle.

Over 2,000 pollinators have been collected and identified on CTMN plots. While identifications are ongoing, 79 species of bees have been identified, including 33 Apidae, 24 Megachilidae, 15 Halictidae, 4 Andrenidae, 2 Colletidae, and 1 Melittidae. Forests play an essential role in conserving pollinating insects and supporting pollination services. Previous works indicate that pollinator abundance and diversity generally increase as forests become more structurally complex but that patterns vary by forest type (Ulyshen et al. 2024). Pollinator communities tend to respond positively to tree mortality, especially in dense conifer forests where herbaceous floral diversity usually increases following tree mortality.

Audley et al. (2025) characterized woodborer and wood decay-related beetle responses to ethanol-baited, panel flight intercept traps on select CTMN plots in 2022 and 2023. A total of 4,077 beetles were captured, spanning 29 families in 2022 with Latridiidae (506), Curculionidae (284), and Cryptophagidae (223) most common and 34 families in 2023 with Elateridae (534), Dermestidae (410), and Curculionidae (308) most common. Individuals spanned 36 woodboring and wood decay-related species in 2022 with fruit-tree pinhole borer (*Xyleborinus saxesenii* [Ratzeburg]; Curculionidae; 216), *Athous* spp. (Elateridae; 48), and a click beetle (*Hemicrepidius obscurus* [LeConte]; Elateridae; 37) most common and 44 woodboring and wood decay-related species in 2023 with fruit-tree pinhole borer (222), *Athous* spp. (146), and another click beetle (*Cardiophorus edwardsi* [Horn]; Elateridae; 95) most common. In general, woodborers were more diverse on plots with high tree mortality than on plots with low mortality. Wood decay beetles were more diverse on plots with high snag fall. The amount of tree mortality and snag fall were positively related to several woodborer and wood decay-related beetles. Woodborers contribute to nutrient cycling, create habitat and/or facilitate access to habitat for insects and other taxa, and are important components of the food web (Dodds et al. 2023).

CONCLUSIONS

The CTMN has been critical in providing an understanding of the effects of tree mortality on forest structure and composition, fuel loads, and fire risk and behavior, as well as pollinator communities and invasive plants. The CTMN shares and leverages data and expertise to better project changes in carbon sequestration and storage, to model silvicultural alternatives for improving forest recovery and to project future forests, and to better understand relationships between water storage and drought stress in seasonally dry forests. Results are widely used by natural resource specialists to inform forest management. A recent publication reported that outbreaks of western pine beetle were incited by the 2012–2015 drought but that the severity of outbreaks and associated tree losses were driven by host density (Robbins et al. 2023). Moving forward, host density can be regulated by mechanical thinning, prescribed fire, and/or managed wildfire (i.e., wildfires that are allowed to burn) where appropriate.

ACKNOWLEDGMENTS

We thank numerous colleagues who have contributed to the California Tree Mortality Network, as well as Christopher Asaro (Forest Service, Forest Health Protection) and Robert Progar (Forest Service, Sustainable Forest Management Research) for their helpful reviews of an earlier version of this summary. This work was supported, in part, by grants from the Pacific Southwest Research Station's Climate Change Program, Support of Long-Term Studies Program, and Initiative Program; the University of California Division of Agriculture and Natural Resources Competitive Grant Program; and EM-WC-21-02 ("Changes in Forest Structure and Composition, Fuel Loads, Pollinator Communities, and Invasive Plant Communities Following Severe Drought in the Central and Southern Sierra Nevada").

For more information, contact: Christopher J. Fettig, christopher.fettig@usda.gov

LITERATURE CITED

Audley, J.P.; Fettig, C.J.; Mortenson, L.A.; Hamud, S.M. 2025. Woodborers and wood-decay related beetle responses to a major forest disturbance event in the central and southern Sierra Nevada, California. Environmental Entomology. 54: 274–286. https://doi.org/10.1093/ee/nvaf014.

Audley, J.P.; Fettig, C.J.; Munson, A.S. [et al.]. 2021. Dynamics of beetle-killed snags following mountain pine beetle outbreaks in lodgepole pine forests. Forest Ecology and Management. 482: 118870. https://doi.org/10.1016/j.foreco.2020.118870.

Brown, J.K. 1974. Handbook for inventorying downed woody material. Gen. Tech. Rep. INT-16. Ogden, UT: U.S. Department of Agriculture, Forest Service, Intermountain Research Station. 24 p.

California Invasive Plant Council. 2024. https://www.cal-ipc.org/plants/profiles/. [Date accessed: July 16, 2024].

Cook, E.R.; Seager, R.; Cane, M.A. [et al.]. 2007. North American drought: reconstructions, causes, and consequences. Earth-Science Reviews. 81: 93–134. https://doi.org/10.1016/j.earscirev.2006.12.002.

Dodds, K.J.; Sweeney, J.; Allison, J.D. 2023. Woodborers in forest stands. In: Allison, J.; Paine, T.D.; Slippers, B.; Wingfield, M.J., eds. Forest entomology and pathology: volume 1: entomology. London: Springer International Publishing: 361–415. https://doi.org/10.1007/978-3-031-11553-0_12.

Fettig, C.J. 2016. Native bark beetles and wood borers in Mediterranean forests of California. In: Lieutier, F.; Paine, T.D., eds. Insects and diseases of Mediterranean forest systems. Switzerland: Springer International Publishing: 499–528. https://doi.org/10.1007/978-3-319-24744-1_18.

Fettig, C.J.; Mortenson, L.A.; Bulaon, B.M.; Foulk, P.B. 2019a. Tree mortality following drought in the central and southern Sierra Nevada, California. U.S. . Forest Ecology and Management. 432: 164–178. https://doi.org/10.1016/j.foreco.2018.09.006.

Fettig, C.J.; Wuenschel, A.; Balachowski, J. [et al.]. 2019b. Managing effects of drought in California. In: Vose, J.; Patel-Weynand, T.; Peterson, D.L.; Luce, C.H., eds. Gen. Tech Rep. WO-98. Effects of drought on forests and rangelands in the United States: translating science into management responses. Washington, DC: U.S. Department of Agriculture, Forest Service: 71–93.

Franceschi, V.R.; Krokene, P.; Christiansen, E.; Krekling, T. 2005. Anatomical and chemical defenses of conifer bark against bark beetles and other pests. New Phytologist. 167: 353–376. https://doi.org/10.1111/j.1469-8137.2005.01436.x.

Hurteau, M.; North, M. 2008. Mixed-conifer understory response to climate, nitrogen, and fire. Global Change Biology. 14: 1543–1552. https://doi/10.1111/j.1365-2486.2008.01584.x.

Kolb, T.E.; Fettig, C.J.; Ayres, M.P. [et al.]. 2016. Observed and anticipated impacts of drought on forests insects and diseases in the United States. Forest Ecology and Management. 380: 321–334. https://doi.org/10.1016/j.foreco.2016.04.051.

Koontz, M.J.; Latimer, A.M.; Mortenson, L.A. [et al.]. 2021. Cross-scale interaction of host tree size and climate governs bark beetle-induced tree mortality. Nature Communications. 12: 129. https://doi.org/10.1038/s41467-020-20455-y.

Luo, L.; Apps, D.; Arcand, S.; [et al.]. 2017. Contribution of temperature and precipitation anomalies to the California drought during 2012–2015. Geophysical Research Letters. 44: 3184–3192. https://doi.org/10.1002/2016GL072027.

Pyke, G.H.; Inouye, D.W.; Thomson, J.D. 2011. Activity and abundance of bumble bees near Crested Butte, Colorado: diel, seasonal, and elevation effects. Ecological Entomology. 36: 511–521. https://doi.org/10.1111/j.1365-2311.2011.01295.x.

Robbins, Z.J.; Xu, C.; Aukema, B.H. [et al.]. 2022. Warming increased bark beetle-induced tree mortality by 30% during an extreme drought in California. Global Change Biology. 28: 509–523. https://doi.org/10.1111/gcb.15927.

Robbins, Z.J.; Xu, C.; Jonko, A. [et al.]. 2023. Carbon stored in live ponderosa pines in the Sierra Nevada will not return to pre-drought (2012) levels during the 21st century due to bark beetle outbreaks. Frontiers in Environmental Science. 11: 1112756. https://doi.org/10.3389/fenvs.2023.1112756.

Stephens, S.L.; Martin, R.E.; Clinton, N.E. 2007. Prehistoric fire area and emissions from California's forests, woodlands, shrublands, and grasslands. Forest Ecology and Management. 251: 205–216. https://doi.org/10.1016/j.foreco.2007.06.005.

Swain, D.L.; Horton, D.E.; Singh, D.; Diffenbaugh, N.S. 2016. Trends in atmospheric patterns conducive to seasonal precipitation and temperature extremes in California. Science Advances. 2: e1501344. https://doi.org/10.1126/sciadv.1501344.

Tappeiner, J.; Radosevich, S. 1982. Effect of bearmat (Chamaebatia foliolosa) on soil moisture and ponderosa pine (Pinus ponderosa) growth. Weed Science. 30: 98–101. https://doi.org/10.1017/S0043174500026254.

Ulyshen, M.; Ballare, K.M.; Fettig, C.J. [et al.]. 2024. The quality of forests to pollinating insects varies with forest structure, composition, and age. Current Forestry Reports. 10: 322–336. https://doi.org/10.1007/s40725-024-00224-6.

Vilanova, E.; Mortenson, L.A.; Cox, L.E. [et al.]. 2023. Characterizing ground and surface fuels across Sierra Nevada forests shortly after the 2012–2016 drought. Forest Ecology and Management. 537: 120945. https://doi.org/10.1016/j.foreco.2023.120945.

White, D.E.; Newton, M. 1989. Competitive interactions of whiteleaf manzanita, herbs, Douglas-fir, and ponderosa pine in southwest Oregon. Canadian Journal of Forest Research. 19: 232–238. https://doi.org/10.1139/x89-032.

Zelikova, T.J.; Hufbauer, R.A.; Reed, S.A. [et al.]. 2013. Eco-evolutionary responses of Bromus tectorum to climate change: implications for biological invasions. Ecology and Evolution. 3: 1374–1387. https://doi.org/10.1002/ece3.542.

CHAPTER 4

Establishing a Monitoring System of Emerald Ash Borer Invasion Impacts on Tribal Black Ash Wetlands

Christel C. Kern, Angela Waupochick, Paul C. Stoy, Sarah Hart, Amy M. Trowbridge, and Anne Timm

How to cite this chapter:

Kern, Christel C.; Waupochick, Angela; Stoy, Paul C.; Hart, Sarah; Trowbridge, Amy M.; Timm, Anne. 2026. Establishing a monitoring system of emerald ash borer invasion impacts on Tribal black ash wetlands. In: Lim-Hing, Simone; Pandit, Karun, eds. Forest Health Monitoring: Evaluation Monitoring project summaries 2024. Gen. Tech. Rep. WO-109a. Washington, DC: U.S. Department of Agriculture, Forest Service: 29–38. Chapter 4.

INTRODUCTION

Globally, wetlands are declining in quantity and quality due to many complex factors, including land use change, climate change, and invasive species (Gardner and Finlayson 2018, Lovett et al. 2016, Mitsch and Hernandez 2013). Invading pests and pathogens, in particular, can significantly alter wetland ecosystem functions, such as nutrient cycling, succession, and hydrology (Lázaro-Lobo and Ervin 2021). Although wetlands represent 1 to 3 percent of land area worldwide, they provide 20 to 30 percent of ecosystem services (Sannigrahi et al. 2018), including habitat for regional biodiversity, controls on biogeochemical cycling, pollutant removal, and floodwater retention. Consequently, loss of wetlands is resulting in major impacts on numerous ecosystem and cultural services (Gardner and Finlayson 2018).

Wetlands are known for their hydrologic functions, which in turn support a range of services critical for ecosystem condition and benefits to local communities. In forested wetlands, the tree layer—the dominant vegetation—influences the water table primarily through transpiration. Surface water levels in forested wetlands peak in spring and drop with leaf out, such as in black ash (*Fraxinus nigra*) wetlands in the Great Lakes region of the United States (Shannon et al. 2018). Individual trees as well as forest composition can affect hydrology and related ecosystem services of forested wetlands; thus, a better understanding of how human-driven disturbances affect the benefits of wetlands may aid managers in creating resilience in these systems.

In North America, the nonnative emerald ash borer (EAB; *Agrilus planipennis*) has been invading ash (*Fraxinus* spp.) forests for nearly two decades. EAB larvae feed within the inner bark and outer sapwood, essentially cutting off the sap flow and transpiration within a tree. Ultimately, EAB infestation results in the mortality of most ash trees (stems >2.5 cm in diameter) and the creation of extensive forest canopy gaps and woody debris (Gandhi and Herms 2010, Herms et al. 2014). EAB invasion in the United States has been in the saturation phase since 2015, suggesting that suitable habitat, largely in uplands, has been invaded (Ward et al. 2020). However, the arrival and establishment of EAB in forested ash wetlands is in earlier stages (Siegert et al. 2023).

A few experimental studies in black ash-dominated wetlands have simulated the impacts of EAB invasion, but there has been little to no research in wetlands that have actually been invaded. In experimental removals of black ash, clearcutting (100 percent) resulted in water tables higher than reference (no cut) conditions, while removing 20 percent of black ash resulted in water levels no different than references (Kolka et al. 2018). Additional research is needed to identify the range of conditions in which black ash regulates wetland hydrology.

For Tribal communities, the impacts of EAB on black ash wetlands are not only ecological but cultural as well. Basketry is a common use of black ash, and the seasonally saturated black ash wetlands grow more suitable trees for basketry than upland or perennially saturated conditions (Benedict and Frelich 2008). In U.S. States with Tribal Nations and black ash populations, 39 of 54

Tribal Nations are located within EAB-invaded counties (Siegert et al. 2023). Near complete EAB invasion of black ash is forecasted between 2035 and 2045, ultimately affecting the culture and livelihoods of all Tribal Nations in northeastern North America (Siegert et al. 2023).

Project Background

The Menominee and Stockbridge-Munsee Community Tribes in northeastern Wisconsin value ash for its ecological services and support of cultural practices and commodities. These Tribal communities were distant from EAB's first U.S. detection in Detroit, MI—over 500 miles away—in 2002. The State of Wisconsin first detected EAB presence in the State in 2008, approximately 125 miles south of these Tribal boundaries. In 2008, statewide restrictions on the movement of ash wood were imposed (Wisconsin DATCP; Wisconsin DNR 2006 [2008 update]). Despite these efforts, EAB was confirmed on lands of both Tribes in 2022. In 2023, 69 of Wisconsin's 72 counties had detected EAB and the State rescinded EAB quarantine rules on the movement of ash wood.

Prior to 2015, there were no active research efforts on the black ash wetlands on Menominee and Stockbridge-Munsee Community lands and only minimal mapping and monitoring of these areas. In addition, extrapolating the few recent studies in Minnesota and Michigan (i.e., Kolka et al. 2018) was difficult because Menominee and Stockbridge-Munsee Community black ash wetlands exhibit very different habitat conditions, namely being composed of mixed species and structured as small wetlands interconnected to large complexes. Given the integral role of black ash in these communities, mitigation and adaptive management strategies were a pressing need to retain the function and services of black ash wetlands. Both Tribes consider black ash wetlands an irreplaceable resource and have prioritized research initiatives aimed at enhancing conservation and mitigation efforts.

Integrated forest pest management was the first step to address the anticipated EAB invasion. Similar to other forest management organizations in the region, the Tribal forestry programs aimed to reduce suitable habitat for EAB through scheduled partial harvests in upland forests when feasible (Menominee Tribal Enterprises 2012 [2018 update]). For lowland forests, harvesting had been prohibited or deferred for decades to protect wetland functions and cultural use. With minimal information on black ash wetland ecology and management, however, passive or no management had continued. Thus, Tribal managers began to seek partnerships to address gaps in knowledge and management practices to sustain black ash wetlands in the face of EAB invasion.

In 2015, the Stockbridge-Munsee Community initiated development of a wetland program intended to support the goals of Tribal water quality management and to begin learning more about their black ash resource. A functional mapping assessment tentatively identified substantial acres of wetlands with black ash components. To initiate monitoring of pre-EAB black ash wetlands, a collaboration was formed in

2017 with the U.S. Department of Agriculture, Forest Service's Northern Research Station.

In 2019, the collaboration between the Northern Research Station and Stockbridge-Munsee Community continued with an Evaluation Monitoring grant from the Forest Service's Forest Health Monitoring (FHM) program. The collaboration and project evolved over the 5-year project period to better serve project and Tribal partnership goals. Initial monitoring included sap flow data collection to investigate and compare transpiration rates among co-occurring canopy species on Stockbridge-Munsee Community lands. Additional details on the sites and initial data collection are described in Waupochick (2023). The project next expanded to include partnership with the University of Wisconsin-Madison and Menominee Indian Reservation. In 2022, the data collection focus shifted from tree-level sap flow to evapotranspiration, which encompasses both tree- and stand-level transpiration (water loss from all vegetation) and surface evaporation (water loss from the soil and other surfaces) as a more comprehensive variable to better address major knowledge gaps around black ash's regulating function at the stand level. To do this, we (the authors of this chapter) applied eddy covariance methods: a micrometeorological technique that enables direct, high-frequency measurements of evapotranspiration from the ecosystem. There are no eddy covariance measurements of EAB-infested stands to date. In the following sections, we provide an overview of the eddy covariance monitoring system and data.

METHODS

Project Area

The project area includes forests on the Menominee Indian Reservation (45°00'11.40" N, -88°42'24.59" W) and Stockbridge-Munsee Community (33°32'39.408" N and -84°14'1.716" E) in northeastern Wisconsin. The study area's physiography, relief, and drainage are primarily the result of glaciation, forming moraines and till. The lowlands are often extensive wetland complexes that include open-water marshes, conifer, and mixed forested wetland types. The average monthly highs and lows in temperature are 24 °F and 5 °F in January and 81 °F and 58 °F in July. The mean annual precipitation is 31 inches (79 cm) with a mean annual snowfall of 48 inches (122 cm) (U.S. Climate Data 2024).

Monitoring Design

Between 2020 and 2022, two guyed metal towers, 80 and 100 feet tall, were installed on Stockbridge-Munsee Community lands. The sites were mixed-species forested wetlands with >30 percent black ash in the overstory and seasonally flooded hydrologic regimes. At the time of installation, EAB presence was detected within 2–4 miles of each site. Tower access and monitoring data are owned by the Tribe but available for research through an agreement.

Sampling

The towers were instrumented to collect high-frequency (10 Hz) measurements of carbon dioxide and water vapor concentrations with

closed-path infrared gas analyzers (Li-7200) and all three components of wind velocity using a sonic anemometer (Campbell Scientific CSAT3) to measure net carbon flux, latent heat flux (from which evapotranspiration can be calculated), and sensible heat flux at 30-minute intervals. In addition, air temperature and relative humidity were measured using HygroVue™5 Temperature and Relative Humidity Sensors (Onset), precipitation was measured using a TE525 Tipping Bucket (Texas Instruments), and photosynthetically active photon flux density was measured using a quantum sensor (CM-230).

Analysis

We calculated half-hourly evapotranspiration from eddy covariance measurements with EddyPro software using double rotation (Kaimal and Finnigan 1994), block averaging, covariance maximization for time lag detection (Foken et al. 2004), and the low- and high-pass filters (Moncrieff et al. 1997, 2004). Spike removal was performed as described by Vickers and Mahrt (1997). Spikes were defined as more than 3.5 standard deviations from the mean mixing ratio for water vapor and carbon dioxide and 5 standard deviations for vertical wind velocity. There were intermittent problems with the infrared gas analyzer pump turning off and not restarting; thus, we prepared a subset of 2023 data from one tower for this report.

RESULTS

The subset of 2023 data from one site showed that evapotranspiration was lower in early spring than summer (May versus July; fig. 4.1) when temperatures were cooler (fig. 4.2C). Evapotranspiration also decreased during cool, cloudy, and rainy periods in June and July (figs. 4.1 and 4.2). Over a 1-month period of contiguous measurements during the late spring/early summer period (June 4 until July 5), 4.5 inches (115 mm) of water were evapotranspired (fig. 4.3).

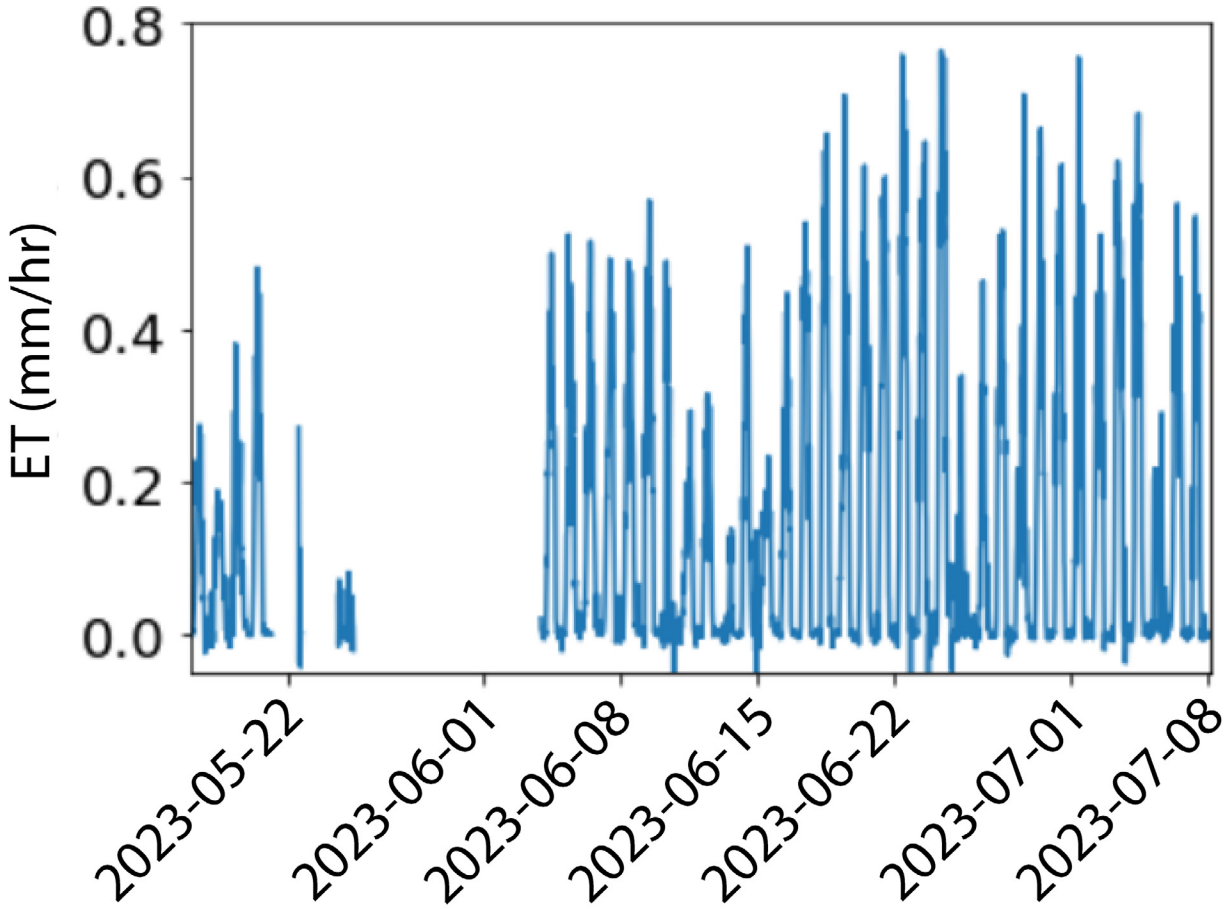

Figure 4.1 —Evapotranspiration (ET) during late spring and early summer 2023 as measured by an eddy covariance tower located in a black ash wetland on Stockbridge-Munsee Community lands, WI.

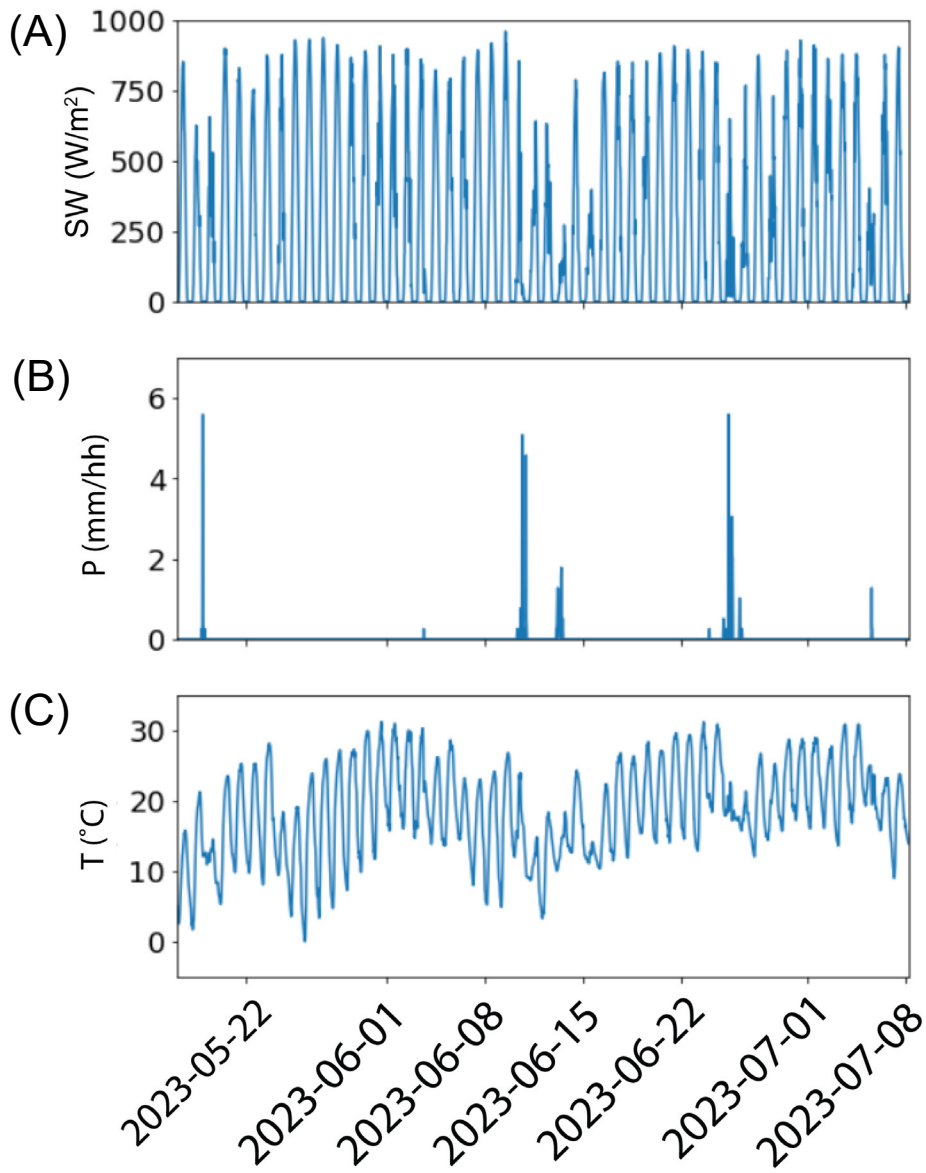

Figure 4.2—(A) Incident shortwave solar radiation (SW), (B) precipitation (P), and (C) air temperature (T) measured above the forest canopy in late spring and early summer 2023 from an eddy covariance tower located in a black ash wetland on Stockbridge-Munsee Community lands, WI.

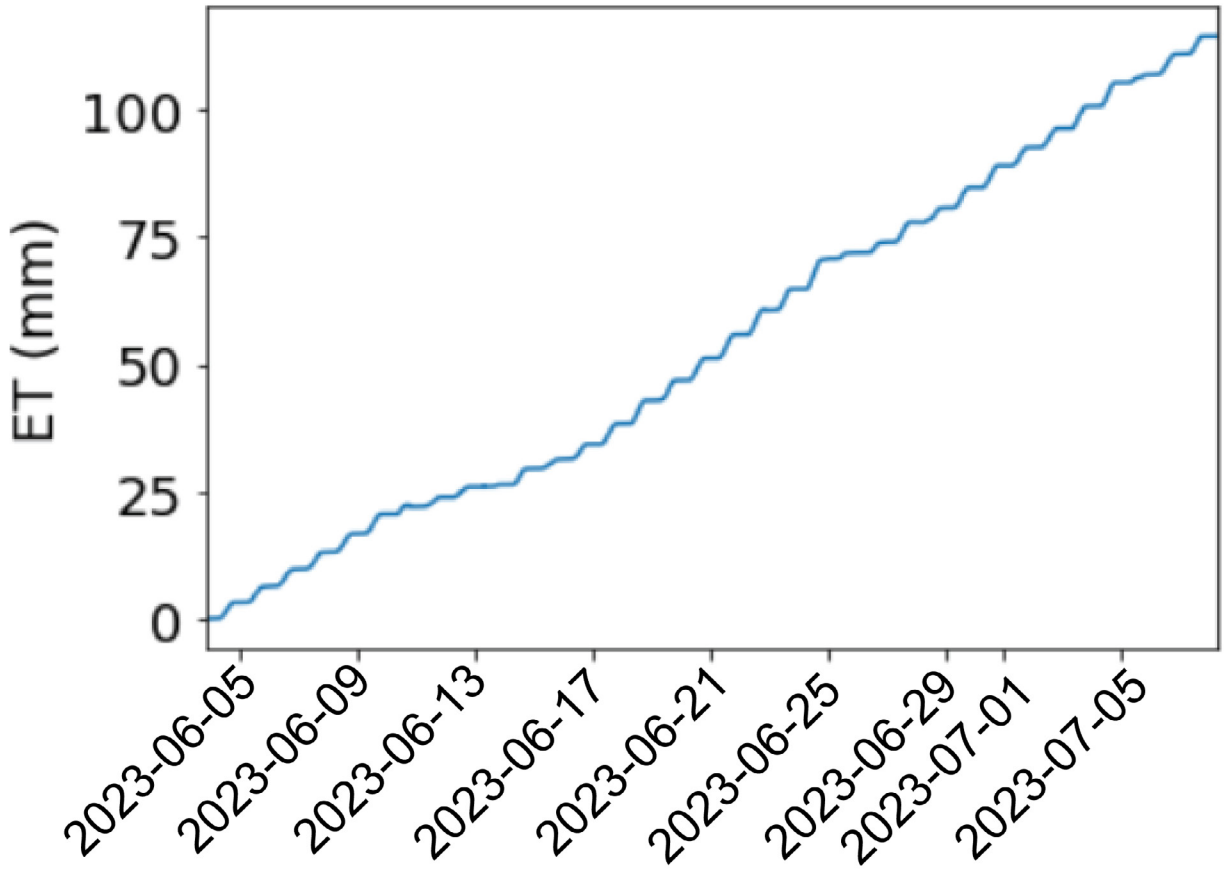

Figure 4.3 —The cumulative sum of evapotranspiration (ET) from early June until early July 2023 as measured by an eddy covariance tower located in a black ash wetland on Stockbridge-Munsee Community lands, WI.

DISCUSSION

Wetlands represent a small portion of the landscape but have exponential ecological and cultural services. In black ash forested wetlands, trees keep water levels and hydrologic processes well moderated. Widespread loss of black ash is expected to drive substantial hydrologic changes by reducing transpiration and affecting wetland functions. For the Menominee and Stockbridge-Munsee Community, the cultural, ecological, and municipal impacts will be multidimensional. Monitoring to understand black ash wetlands on Tribal lands and specifically the regulating role of black ash in hydrologic functions were primary goals of this Evaluation Monitoring project.

Presenting a subset of data in this chapter is the first step to developing baseline observations of black ash wetland hydrologic functions before visible EAB disturbance is present. Based on this initial data collection, nearly 5 inches of water were transpired in June of 2023. Other research has shown that black ash trees transpire significantly more than co-occurring species (Shannon et al. 2018) and transpire large amounts of water, up to 16 gallons per day (Telander et al. 2015). Thus, black ash mortality from wetlands could result in significantly less water lost through transpiration and more water redistributed as extended periods of surface water or flooding, depending on weather and site conditions. Evapotranspiration will likely increase over summers as temperatures and solar radiation increase, but cool, rainy summers could have the opposite effect. Differences in site hydrology will also likely alter the outcomes of black ash mortality. In sites influenced by ground water, water table depth may not substantially change when transpiration is reduced following black ash mortality. Longer term data are needed to understand seasonal and interannual variation.

CONCLUSIONS

The Tribes continue to be concerned about the impact of EAB as it relates to the loss of black ash trees and the increased potential for perennial surface waters and flooding to have negative impacts on infrastructure and available habitat, as well as conversion to nonforest types and increased management and staffing needs. As such, the Stockbridge-Munsee Community and University of Wisconsin signed a Memorandum of Understanding in January 2024 (expiration 2029) to continue the eddy covariance monitoring system that was established with the contributions from FHM funding. This Memorandum of Understanding aims to build a long-term dataset of baseline data in these wetlands and track the impacts of EAB invasion, black ash mortality, and response of co-occurring species. The long-term monitoring will also produce a more complete understanding of the hydrology and will be a basis for forecasting the potential impacts of EAB impacts on black ash wetlands on Tribal lands and beyond.

ACKNOWLEDGMENTS

We thank the forestry and natural resource staff and leaders at Stockbridge-Munsee Community and Menominee Tribal Enterprises for their support through all phases of this project. We also thank Dave Mausel and Dan Cornelius for their comments on an earlier version of this manuscript. This project was funded by the Evaluation Monitoring program of Forest Service Forest Health Monitoring, College of Agricultural and Life Sciences at the University of Wisconsin-Madison, National Science Foundation Division of Environmental Biology award 2106012, and University of Wisconsin-Madison Office of the Vice Chancellor for Research and Graduate Education with funding from the Wisconsin Alumni Research Foundation.

For more information, contact: Christel Kern, christel.c.kern@usda.gov

LITERATURE CITED

Benedict, M.; Frelich, L. 2008. Site factors affecting black ash ring growth in northern Minnesota. Forest Ecology and Management. 255: 3489–3493. https://doi.org/10.1016/j.foreco.2008.02.029.

Foken, T.; Göockede, M.; Mauder, M. [et al.]. 2004. Post-field data quality control. In: Lee, X.; Massman, W.; Law, B., eds. Handbook of micrometeorology. Atmospheric and Oceanographic Sciences Library. Dordrecht: Springer Netherlands: 181–208. https://doi.org/10.1007/1-4020-2265-4_9.

Gandhi, K.; Herms, D. 2010. Direct and indirect effects of alien insect herbivores on ecological processes and interactions in forests of eastern North America. Biological Invasions. 12: 389–405. https://doi.org/10.1007/s10530-009-9627-9.

Gardner, R.C.; Finlayson, C. 2018. Global wetland outlook: state of the world's wetlands and their services to people. Ramsar Convention Secretariat. Stetson University College of Law. 89 p.

Herms, D.; McCullough, D.; Berenbaum, M. 2014. Emerald ash borer invasion of North America: history, biology, ecology, impacts, and management. Annual Review of Entomology. 59: 13–30. https://doi.org/10.1146/annurev-ento-011613-162051.

Kaimal, J.C.; Finnigan, J.J. 1994. Atmospheric boundary layer flows: their structure and measurement. New York: Oxford University Press. 289 p. https://doi.org/10.1093/oso/9780195062397.001.0001.

Kolka, R.; D'Amato, A.; Wagenbrenner, J. [et al.]. 2018. Review of ecosystem level impacts of emerald ash borer on black ash wetlands: what does the future hold? Forests. 9: 179. https://doi.org/10.3390/f9040179.

Lázaro-Lobo, A.; Ervin, G. 2021. Wetland invasion: a multi-faceted challenge during a time of rapid global change. Wetlands. 41: 65. https://doi.org/10.1007/s13157-021-01462-1.

Lovett, G.; Weiss, M.; Liebhold; A.. [et al.]. 2016. Nonnative forest insects and pathogens in the United States: impacts and policy options. Ecological Applications. 26: 1437–1455. https://doi.org/10.1890/15-1176.

Menominee Tribal Enterprises. 2012 (2018 update). Emerald ash borer plan. Keshena, WI. https://www.mtewood.com/SustainableForestry/EABPlan. [Date accessed: September 12, 2025].

Mitsch, W.; Hernandez, M. 2013. Landscape and climate change threats to wetlands of North and Central America. Aquatic Sciences. 75: 133–149. https://doi.org/10.1007/s00027-012-0262-7.

Moncrieff, J.; Clement, R.; Finnigan, J.; Meyers, T. 2004. Averaging, detrending, and filtering of eddy covariance time series. In: Lee, X.; Massman, W.; Law, B., eds. Handbook of micrometeorology. Atmospheric and Oceanographic Sciences Library. Dordrecht: Springer Netherlands: 7–31. https://doi.org/10.1007/1-4020-2265-4_2.

Moncrieff, J.; Massheder, J.; deBruin, H. [et al.]. 1997. A system to measure surface fluxes of momentum, sensible heat, water vapour and carbon dioxide. Journal of Hydrology. 188: 589–611. https://doi.org/10.1016/S0022-1694(96)03194-0.

Sannigrahi, S.; Bhatt, S.; Rahmat, S. [et al.]. 2018. Estimating global ecosystem service values and its response to land surface dynamics during 1995–2015. Journal of Environmental Management. 223: 115–131. https://doi.org/10.1016/j.jenvman.2018.05.091.

Shannon, J.; Van Grinsven, M.; Davis, J. [et al.]. 2018. Water level controls on sap flux of canopy species in black ash wetlands. Forests. 9: 147. https://doi.org/10.3390/f9030147.

Siegert, N.; McCullough, D.; Luther, T. [et al.]. 2023. Biological invasion threatens keystone species indelibly entwined with Indigenous cultures. Frontiers in Ecology and the Environment. 21: 310–316. https://doi.org/10.1002/fee.2654.

Telander, A.; Slesak, R.; D'Amato, A. [et al.]. 2015. Sap flow of black ash in wetland forests of northern Minnesota, USA: hydrologic implications of tree mortality due to emerald ash borer. Agricultural and Forest Meteorology. 206: 4–11. https://doi.org/10.1016/j.agrformet.2015.02.019.

U.S. Climate Data. 2024. Climate Shawano - Wisconsin. U.S. Climate Data 2024 – version 3.0. https://www.usclimatedata.com/climate/shawano/wisconsin/united-states/uswi0628. [Date accessed: June 12, 2024].

Vickers, D.; Mahrt, L. 1997. Quality control and flux sampling problems for tower and aircraft data. Journal of Atmospheric and Oceanic Technology. 14: 512–526. https://doi.org/10.1175/1520-0426(1997)014<0512:QCAFSP>2.0.CO;2.

Ward, S.; Fei, S.; Liebhold, A. 2020. Temporal dynamics and drivers of landscape-level spread by emerald ash borer. Journal of Applied Ecology. 57: 1020–1030. https://doi.org/10.1111/1365-2664.13613.

Waupochick, A. 2023. Anticipating the hydrological consequences of emerald ash borer in tribal forests. Madison, WI: University of Wisconsin-Madison. 44 p. M.S. Thesis.

Wisconsin Department of Agriculture, Trade, and Consumer Protection [DATCP]; Wisconsin Department of Natural Resources [DNR]. 2006 (2008 update). Wisconsin emerald ash borer response plan. Madison, WI. 30 p.

CHAPTER 5

The Impacts of an Exceptional Drought on Forests in Eastern Texas: Disparities in Tree Mortality, Biomass Loss, and Decrease in the Carbon Sink Capacity

Weimin Xi, Mukti Ram Subedi, Tilak Chaudhary, Nicholas P. Dewez, Duston R. Duffie, Roshan P. Bhatta, Zhiping Liu, Qingqing Liu, Xiaoyu Liu, Yanmei Chen, Ming Yan, Sandra Rideout-Hanzak, Ambrose O. Anoruo, Haibin Su, and Stephen Clarke

INTRODUCTION

Drought is an insidious natural disturbance and has been a constant threat to environmental and anthropogenic prosperity. Increasing drought severity has increased tree mortality and biomass loss worldwide, significantly altering forest structure, species composition, successional dynamics, carbon and energy fluxes, and ecosystem services (Clark et al. 2016, Turner 2010). The effects of severe and lasting drought are and will continue to be confounded and complex, potentially reducing resilience of forest ecosystems and pushing them over a tipping point to an alternate steady state of forest succession (Anderegg et al. 2015, Trenberth et al. 2013).

Texas has experienced several cycles of major droughts over the last century (Nielsen-Gammon 2012). The exceptional 2011 drought killed approximately 301 million trees statewide, including 65 million trees in eastern Texas alone (Moore et al. 2016). Climate projections for Texas suggest increased tree mortality through drought and insect attacks, with manifold impacts on forests (Nielsen-Gammon et al. 2020, Seidl et al. 2017). The importance of drought in eastern Texas has long been recognized, and studies have largely focused both on the short-term and stand-level impacts on forested ecosystems. However, the long-term and cyclical nature of the disturbance at the landscape scale and its relationship to climate scenarios have not been fully explored.

This study aimed to investigate the effects of the exceptional 2011 drought on tree mortality, biomass loss, and carbon dynamics, as well as their spatiotemporal variations in eastern Texas. We (the authors of this chapter) used 20 years of plot-level Nationwide Forest Inventory data from the Forest Inventory and Analysis (FIA) program. Our objectives were to: (1) examine drought-induced tree mortality rates by separating drought from other damaging agents attributable to tree mortality; (2) investigate the spatiotemporal variations of drought with stand condition, age, and crown conditions; and (3) develop a spatially referenced prediction of drought severity and forest condition maps under different projected climate scenarios.

How to cite this chapter:

Xi, Weimin; Subedi, Mukti Ram; Chaudhary, Tilak; Dewez, Nicholas P.; Duffie, Duston R.; Bhatta, Roshan P.; Liu, Zhiping; Liu, Qingqing; Liu, Xiaoyu; Chen, Yanmei; Yan, Ming; Rideout-Hanzak, Sandra; Anoruo, Ambrose O.; Su, Haibin; Clarke, Stephen. 2026. The impacts of an exceptional drought on forests in eastern Texas: disparities in tree mortality, biomass loss, and decrease in the carbon sink capacity. In: Lim-Hing, Simone; Pandit, Karun, eds. Forest Health Monitoring: Evaluation Monitoring project summaries 2024. Gen. Tech. Rep. WO-109a. Washington, DC: U.S. Department of Agriculture, Forest Service: 39–48. Chapter 5.

METHODS

Study Areas

We carried out our studies in eastern Texas at three spatial scales: (1) the four national forests of Texas: Angelina, Davy Crockett, Sabine, and Sam Houston National Forests (sizes ranging from 62,000 to 66,000 ha); (2) the central eastern Texas region; and (3) the entire eastern Texas region (8.96 million ha) (fig. 5.1). Eastern Texas has a mild, mid-latitude, humid subtropical climate with hot summers and mild winters. Many areas have a thick, underlying clay pan with Alfisols and Vertisols, with udic and ustic soil moisture regimes. The region experiences frequent, diverse, and large natural disturbances, including droughts, hurricanes, wildfires, insect outbreaks, and disease. In recent years, invasive species and climate stress have been considered threats to forest health.

The forests of eastern Texas cover an area of 4.9 million ha. Slightly more than 50 percent of the forested area is hardwood forest. Oak-hickory (*Quercus* spp./*Carya* spp.) is the dominant hardwood type, followed by oak-pine (*Quercus* spp./*Pinus* spp.) mixed, and oak-gum-cypress (*Quercus* spp./*Nyssa* spp./*Taxodium distichum*) forest types. Mixed forests of oak-pine cover an estimated 25 percent of forest lands. In softwood forests, loblolly pine (*P. taeda*; 37 percent) and shortleaf pine (*P. echinata*; 3 percent) are the dominant stand types. Of these softwood forests, 40 percent are managed pine plantations. In eastern Texas, ~98 percent of the forest land is timberland and ~92 percent is privately owned. About 8 percent of forested land is public, including four national forests managed by the U.S. Department of Agriculture, Forest Service.

Data

To examine tree mortality, biomass loss, and carbon dynamics at three spatial scales, we utilized FIA data collected between 2001 and 2019 consisting of four complete inventories. In total, we selected 1,797 forest plots from nearly 4,000 plots in eastern Texas. For our analysis within the 4 national forests, we selected 264 plots to examine tree mortality, stand resistance, and carbon loss affected by the drought. For each plot, we compiled stand conditions including stand type, age, density, and basal area from the FIA data. We divided trees according to different ecoregions and forest types to further understand their response to drought. We quantified changes in tree mortality, growth, recruitment, biomass, and carbon losses due to increased drought severity at the three scales. We created current forest condition maps based on recent FIA plot data for the central eastern Texas region and used these as initial community input for our simulation modeling framework.

We obtained historical climate data for the region from the National Oceanic and Atmospheric Administration's (NOAA) National Centers for Environmental Information. We evaluated four geostatistical interpolation methods for spatiotemporal analysis of drought patterns. Using 40 years of climate data, we calculated a 12-month average meteorological drought index, SPEI (Standardized Precipitation Evapotranspiration Index), for each plot and

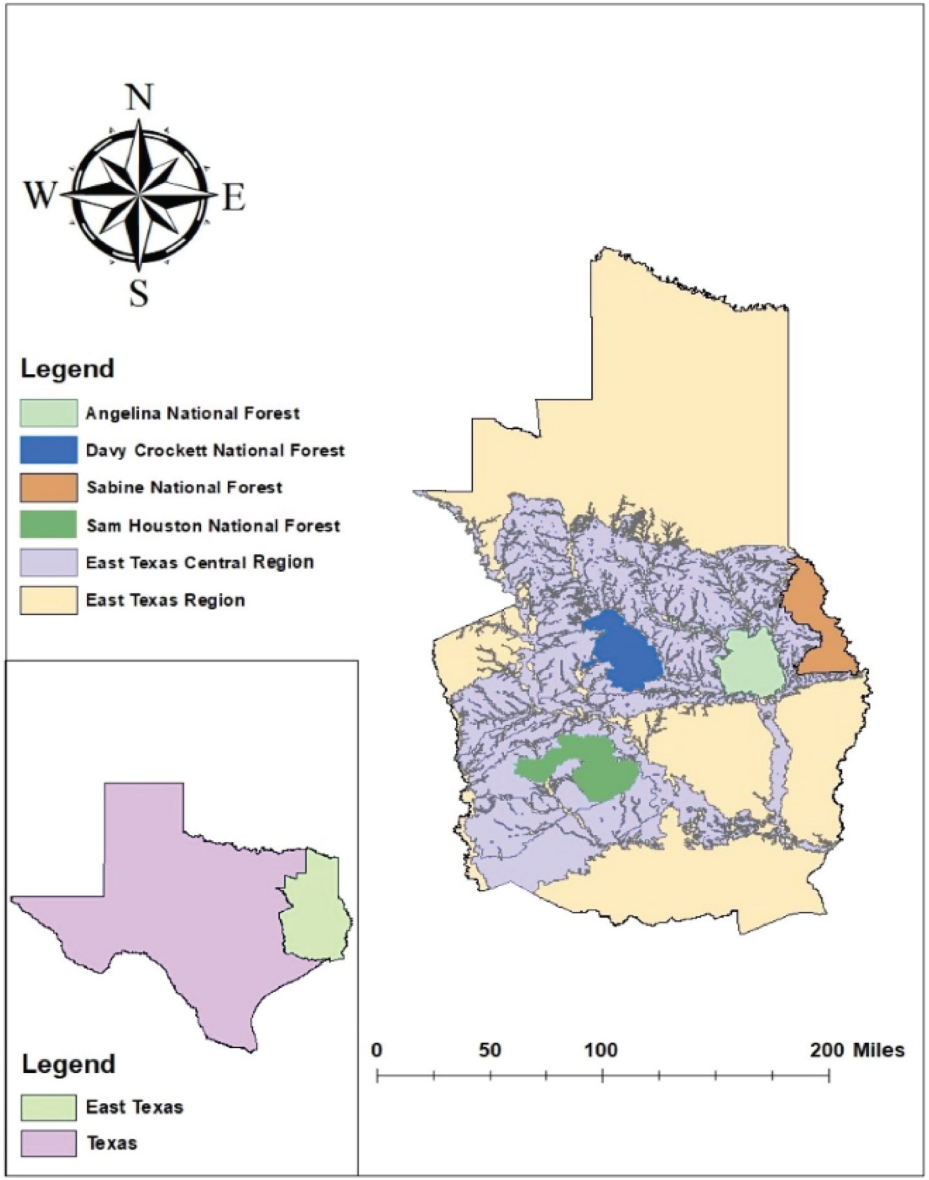

Figure 5.1 — Location map of the four national forests, the central eastern Texas region, and the entire eastern Texas region. National forests include Angelina National Forest, Davy Crockett National Forest, Sabine National Forest, and Sam Houston National Forest.

survey year throughout the monitoring period. We determined drought duration (number of months in severe drought [SPEI <-2.0]) and categorized 20 years of time-series FIA plots into four periods: (1) base (2001–2003), (2) pre-drought (2004–2010), (3) drought (2011–2016), and (4) post-drought (2017–2019). All plots were classified into three groups (no drought, moderate, or severe drought) using cluster analysis on SPEI. We also obtained climate projection data from the U.S. Geological Survey's Geo Data Portal.

Statistical Analyses and Forest Modeling

We selected density-independent factors and density-dependent factors to explore drought-triggered tree mortality. Generalized nonlinear mixed models, principal component analysis, and random forest models were used to examine trends in tree mortality, recruitment, and the relative contribution of influencing factors, including climatic factors (drought severity, drought duration, mean annual temperature, and mean annual precipitation) and stand factors (basal area, stand density, and stand age) in annual and inventory-cycle tree mortality patterns. We analyzed the relative contributions of climatic and stand factors at geographic region, tree species group, tree sizes, height class, and forest stand origin type. For the four national forests, we analyzed temporal and spatial variations of the forest carbon stock at the inventory cycle level and annual level for the pre- and post-drought periods. Moreover, we used repeated measures analysis of variance to analyze annual mortality, biomass loss, growth rates, and the Forest Stability Index to understand the effects of the 2011 drought on mortality, biomass, and growth and to explore forest stability at species, forest, and ecoregion levels. Mortality models were selected based on several criteria such as Akaike information criterion (AIC), Bayesian information criterion (BIC), log-likelihood ratio value (-2logL), mean absolute error (MAE), and root mean square error (RMSE).

We integrated LANDIS-II, a spatially explicit, stochastic model of forest landscape dynamics, as a core model with the newly improved drought extension. This simulates drought effects under future climate scenarios to forecast changes in tree aboveground biomass in the four national forests and surrounding areas of central eastern Texas through the end of the century (2019–2099) and validates simulation results with FIA plot data (Scheller et al. 2007, Xi et al. 2009). We compared two Representative Concentration Pathways (RCPs) against baseline scenarios: (1) business as usual (BAU), (2) low carbon emissions (RCP2.6), and (3) high carbon emissions (RCP8.5).

RESULTS AND DISCUSSION

Widespread Increase in Tree Mortality and Biomass Loss but Disparity in Tree Resistance

Our analyses indicated a widespread increase in tree mortality (corresponding decreases in biomass and carbon loss) across tree sizes, dominant genera, height classes, and ecoregions at all three spatial scales (Chaudhary et al. 2022; Dewez et al. 2024; Subedi et al. 2020; Yan et al. 2022a, 2022b, 2024a, 2024b). An average mortality rate of 5.89 percent per year during the drought period could be attributed to continuous collective impacts due to the extreme 2011 drought and by water stress created by the regional prolonged and episodic drought events. Results demonstrated that *Pinus* spp. suffered the least. The mortality rate of pines (2.1 percent) was lower than that of hardwood species (3.9 percent), while tree mortality in public forest lands (3.0 percent) was higher than that in pine plantations (1.9 percent). The mortality rate of trees in the Western Gulf Coastal Plain ecoregion and southwestern region of eastern Texas was highest after drought.

Tree mortality showed mixed results in terms of the basal area and forest density classifications, either combining all plots together or when analyzing the plots by stand origin and ecoregion. Higher mortality rates of smaller trees were detected in both natural and plantation forests and were likely compounded by density-dependent factors. The effects of drought were more significant on natural forests than on plantation forests. The overall plot recruitment rates decreased during the drought period. Annual growth rates declined by 51 percent in 2011 and by ~23 percent during the inventory cycle with severe drought.

Tree Mortality Risk Factors and the Optimal Predictive Models

Regression analysis of forest density and tree mortality did not illustrate a significant relationship, suggesting that tree mortality was triggered by density-independent factors. Our analyses showed that tree mortality varied with the drought index distribution pattern. The number of dead trees increased as the intensity of the drought and mean summer temperature rose, whereas values decreased as mean summer precipitation increased. Both drought severity and duration of drought had significant negative effects on tree survival, while annual precipitation had a significant positive effect. The results of the principal component analysis showed that the effect of drought was greater than that of tree competition and other natural disturbances, and the effects of drought severity and duration on tree mortality were similar (table 5.1). Our results suggest that it is essential to consider the relative importance of both intrinsic (tree size) and extrinsic (stand and climate) factors in analyzing tree mortality. There were no apparent effects of elevation or latitude on tree mortality.

Among all base-count models, the zero-inflated negative binomial mixed model had the best fit in eastern Texas. In the future, comparative analysis of drought-induced tree mortality using hydrometeorological data along with a drought

Table 5.1—Loading and contribution of three principal components by drought and competition in eastern Texas during drought period (inventory cycle 9, 2009–2013)

Drought and competition variables	Principal component		
	1	2	3
Drought severity	-0.906	-0.008	0.084
Drought length	0.907	0.018	-0.075
Density	-0.118	0.657	-0.648
Basal area	-0.037	0.897	0.13
Stand age/(year)	0.078	0.348	0.874
Remeasurement period/(year)	0.192	0.313	0.023
Eigenvalues	1.701	1.456	1.214
Contribution rate (%)	28.356	24.266	20.241
Cumulative rate (%)	28.356	52.622	72.863

severity and duration gradient could improve understanding of the effects of drought on tree mortality and biomass loss in eastern Texas and within the Southeastern United States.

Strong Resilience to Exceptional Drought and Post-Drought Recovery

Our results showed that while tree mortality and biomass loss increased significantly and annual growth rates declined during the drought period, tree mortality and biomass loss rates returned to pre-drought levels and growth partially recovered during the post-drought period. During the drought period, the Forest Stability Index, defined as the ratio of observed to maximum theoretical tree density, dropped at the species, forest type, and ecoregion levels but recovered during the post-drought period, except for the Oak Woods and Prairies ecoregion and for forests dominated by southern red oak (*Q. falcata*).

Our results indicate that eastern Texas forests are undergoing a reorganization and recovery stage (in terms of species composition and stand structure) but have yet to reach a tipping point. Given the increased frequency and severity of weather-related disturbances, eastern Texas forests could approach a tipping point in the future if there is not enough time between events for reorganization and recovery (Chaudhary et al. 2022).

Changes in Carbon Stock

Our results showed that carbon loss increased significantly in the four national forests due to the 2011 drought and demonstrated covariation with SPEI (Yan et al. 2024b). Carbon loss in the post-drought inventory cycle increased significantly (91.45 t), which was twofold of what was estimated during the inventory cycle before the drought. In the four classification criteria (forest origin, tree size, height classes, and tree species group), carbon loss increased along with increases of drought severity during the drought period. Compared to plantations (2.9 percent), the carbon loss in natural forests was greater (7.4 percent). The carbon loss of smaller trees and shorter trees was 18.7 and 7.9 percent, respectively.

Among different types of forests, pine forests were least affected by the exceptional drought and had the lowest carbon loss (5.1 percent), demonstrating a strong tolerance to drought. Compared to forest stand factors, drought was the dominant factor driving carbon loss rate. The results of random forest models showed that the relative importance score of the severity of drought on carbon loss rate was the highest (9.2 percent, $p < 0.01$) and the relative importance score for the duration of the drought was 8.1 percent ($p < 0.05$). When SPEI <-1.2, the carbon loss rate increased along with increasing drought severity. The relative importance of stand density, tree basal area, and stand age was 4.4, 3.0, and 1.3 percent, respectively.

Future Impacts on Forest Aboveground Biomass

Our simulation results from the LANDIS-II model for the forest lands of the central eastern Texas region showed that total aboveground biomass is projected to increase 0.1 to 8.9 percent under all climate scenarios. Drought and exceptional drought scenarios reported lower increases in aboveground biomass (1.0 to 4.4 percent lower, respectively) compared to the BAU scenarios over our simulation horizon. Without disturbance, RCP2.6 and RCP8.5 scenarios respectively reported 14 and 17 percent lower aboveground biomass than BAU. Although the major results can be applied regionally, more comprehensive data mining and simulations including more multiple damaging factors (e.g., hurricanes, fires, and insect outbreaks) and forest management in eastern Texas under global future climate scenarios could be further studied. Our results suggest that the effects of drought on forest dynamics are complex with potential long-term ecological impacts.

CONCLUSIONS

The analyses of longitudinal Nationwide Forest Inventory data at three spatial scales showed that the 2011 drought had complex and profound impacts on the main aspects of forests in eastern Texas. We found a widespread, varied, and long-lasting increase in tree mortality across eastern Texas forests triggered by the exceptional drought coupled with mortality from wildfire and insect damage (Subedi et al. 2020). In general, the effects of drought on tree mortality are greater than that of competition. The causes of overall tree mortality patterns are complex across a myriad of factors including geographical region, stand origin, tree size, and species (Chaudhary et al. 2022; Yan et al. 2022a, 2022b).

We concluded that 1) *Pinus* spp. is more tolerant to drought than others; 2) the effect of drought was more pronounced on smaller diameter and shorter trees; 3) drought-triggered mortality in natural forests is more severe than in plantation forests; and 4) compared to competition, drought severity and duration together were the leading causes of tree mortality. Annual mortality rates during and after the drought showed a significantly positive correlation with drought severity and duration. The forests of eastern Texas demonstrated resistance to drought and resiliency toward exceptional drought over our 80-year simulations.

Drought events are a common occurrence in nature and play a significant role in the dynamics of forest ecosystems. Gaining a comprehensive understanding of drought's complexity, driving factors under climate conditions with varying

stand conditions, and effects on tree mortality, biomass loss, forest dynamics, carbon stocks, and forest response, is crucial (Dewez et al. 2024; Edgar et al. 2019; Klockow et al. 2020; Liu et al. 2025; Yan et al. 2024a, 2024b). This knowledge can aid landowners, natural resource managers, and those involved in biodiversity conservation and ecosystem management in developing effective forest management strategies to mitigate negative impacts on forest sustainability in eastern Texas and beyond.

ACKNOWLEDGMENTS

The Forest Service's Forest Health Monitoring grant (19-DG-11083150-030) funded this project. We thank Dr. Audrey Barker-Plotkin (Harvard University, Harvard Forest) and Dr. Morgan Leigh Artemam (Forest Service, Southern Research Station, Eastern Forest Environmental Threat Assessment Center) for helpful comments on this manuscript.

For more information, contact: Weimin Xi, weimin.xi@tamuk.edu

LITERATURE CITED

Anderegg, W.R.; Hicke, J.A.; Fisher, R.A. [et al.]. 2015. Tree mortality from drought, insects, and their interactions in a changing climate. New Phytologist 208 (3): 674–863. https://doi.org/10.1111/nph.13477.

Chaudhary, T.; Xi, W.; Subedi, M. [et al.]. 2022. East Texas forests show strong resilience to exceptional drought. Forestry: An International Journal of Forest Research. 96 (3): 326–339. https://doi.org/10.1093/forestry/cpac050.

Clark, J.S.; Iverson, L.; Woodall, C.W. [et al.]. 2016. The impacts of increasing drought on forest dynamics, structure, and biodiversity in the United States. Global Change Biology. 22 (7): 2329–2352. https://doi.org/10.1111/gcb.13160.

Dewez, N.; Xi, W.; Duffie, D. [et al.]. 2024. Analysis of forest inventory data shows disparity in tree mortality and resistance in Texas national forests. Journal of Forestry. 122 (3): 232–243. https://doi.org/10.1093/jofore/fvad059.

Edgar, C.B.; Westfall, J.A.; Klockow, P.A. [et al.]. 2019. Interpreting effects of multiple, large-scale disturbances using national forest inventory data: a case study of standing dead trees in east Texas, USA. Forest Ecology and Management. 437: 27–40. https://doi.org/10.1016/j.foreco.2019.01.027.

Klockow, P.A.; Edgar, C.B.; Moore, G.W.; Vogel, J.G. 2020. Southern pines are resistant to mortality from an exceptional drought in east Texas. Frontiers in Forests and Global Change. 3: 23. https://doi.org/10.3389/ffgc.2020.00023.

Liu, Z.P; Xi, W.; Subedi, M.R. [et al.]. 2025. The impacts of large-scale climate extremes on aboveground biomass in subtropical pine-dominant forests of Texas, USA: 20 years of monitoring. Journal of Forestry Research. 36: 83. https://doi.org/10.1007/s11676-025-01872-5.

Moore, G.W.; Edgar, C.B.; Vogel, J.G. [et al.]. 2016. Tree mortality from an exceptional drought spanning mesic to semiarid ecoregions. Ecological Applications. 26(2): 602–611. https://doi.org/10.1890/15-0330.

Nielsen-Gammon, J.W. 2012. The 2011 Texas drought. Texas Water Journal, 3(1): 59–95. https://doi.org/10. 21423/twj.v3i1.6463.

Nielsen-Gammon, J.W.; Banner, J.; Cook, B. [et al.]. 2020. Unprecedented drought challenges for Texas water resources in a changing climate: What do researchers and stakeholders need to know? Earth's Future. 8: e2020EF001552. https://doi.org/10.1029/2020EF001552.

Scheller, R.M.; Domingo, J.B.; Sturtevant, B.R. [et al.]. 2007. Design, development, and application of LANDIS-II, a spatial landscape simulation model with flexible temporal and spatial resolution. Ecological Modelling, 201(3–4): 409–419. https://doi.org/10.1016/j.ecolmodel.2006.10.009.

Seidl, R.; Thom, D.; Kautz, M. [et al.]. 2017. Forest disturbances under climate change. Nature Climate Change. 7: 395–402. https://doi.org/10.1038/nclimate3303.

Subedi, M.R.; Xi, W.; Edgar, C.B. [et al.]. 2020. Tree mortality and biomass loss in drought-affected forests of east Texas, USA. Journal of Forestry Research. 32(1): 67–80. https://doi.org/10.1007/s11676-020-01106-w.

Trenberth, K.; Dai, A.; Schrier, G. [et al.]. 2013. Global warming and changes in drought. Nature Climate Change. 4: 17–22. https://doi.org/10.1038/nclimate2067.

Turner, M. 2010. Disturbance and landscape dynamics in a changing world. Ecology. 91: 2833–2849. https://doi.org/10.1890/10-0097.1.

Xi, W.; Coulson, R.N.; Birt, A.G. [et al.]. 2009. Review of forest landscape models: types, methods, development and applications. Acta Ecologica Sinica. 29: 69–78. https://doi.org/10.1016/j.chnaes.2009.01.001.

Yan, M.; Chen, Y.; Yan, J.; Xi, W. 2024a. Studying forest tree mortality based on a generalized linear mixed-effects model. Acta Ecologica Sinica. 44(6): 2420–2436 (in Chinese). https://doi.org/10.5846/stxb202304270878.

Yan, M.; Liu, Q.Q.; Liu, Z.P.; Xi, W. 2022a. Impacts of drought and stand factors on tree mortality: a case study of national forests in east Texas, USA. Chinese Journal of Applied Ecology. 33(11): 2897–2906 (in Chinese). https://doi.org/10.13287/j.1001-9332.202211.002.

Yan, M.; Liu, X.Y.; Liu, Q.Q. [et al.]. 2024b. Post-drought carbon dynamics and driving factors in East Texas national forests, USA. Chinese Journal of Ecology. 43(2): 395–406 (in Chinese). https://doi.org/10.13292/j.1000-4890.202402.039.

Yan, M.; Liu, Z.P.; Subedi, M.R. [et al.]. 2022b. The complex impacts of unprecedented drought on forest tree mortality: a case study of dead trees in east Texas, USA. Acta Ecologica Sinica. 42(3): 1034–1046 (in Chinese). https://doi.org/10.5846/stxb202101150152.

ACKNOWLEDGMENTS

This research presented in this report was supported in part through the project "Forest Health Monitoring and Assessment" of Cost Share Agreement 23-CS-11330180-068 (August 30, 2023, through current) between North Carolina State University (this institution is an equal opportunity provider) and the Forest Service, Southern Research Station, Asheville, NC. The Southern Research Station provided funds that supported this research.

The editors and authors of this report thank the following for their reviews and constructive comments: Morgan Leigh Arteman, Chris Asaro, Audrey Barker-Plotkin, Dan Cornelius, Joel M. Egan, Daniel Ott, Robert Progar, and Dave Mausel.

AUTHOR INFORMATION

Ambrose O. Anoruo, Professor of Agriculture and Environmental Sciences, Texas A&M University-Kingsville, Department of Agriculture, Agribusiness, and Environmental Sciences, Kingsville, TX 78363

Jackson P. Audley, Postdoctoral Scholar, U.S. Department of Agriculture, Forest Service, Pacific Southwest Research Station, Vallejo, CA 94592

Roshan P. Bhatta, Graduate Research Assistant, Texas A&M University-Kingsville, Department of Biological and Health Sciences, Kingsville, TX 78363

Beverly M. Bulaon, Entomologist, U.S. Department of Agriculture, Forest Service, Forest Health Protection, Sonora, CA 95370

Michael J. Campbell, Research Assistant Professor, University of Utah, School of Environment, Society, and Sustainability, Salt Lake City, UT 84112

Tilak Chaudhary, Graduate Research Assistant, Texas A&M University-Kingsville, Department of Biological and Health Sciences, Kingsville, TX 78363

Yanmei Chen, Graduate Research Assistant, Shanxi Normal University, School of Life Sciences, Taiyuan 030031, China

Stephen Clarke, Entomologist, U.S. Department of Agriculture, Forest Service, Forest Health Protection, Lufkin, TX 75901

Nicholas P. Dewez, Graduate Research Assistant, Texas A&M University-Kingsville, Department of Biological and Health Sciences, Kingsville, TX 78363

Duston R. Duffie, Graduate Research Assistant, Texas A&M University-Kingsville, Department of Animal, Rangeland, and Wildlife Sciences, Caesar Kleberg Wildlife Research Institute, Kingsville, TX 78363

Christopher J. Fettig, Research Entomologist, U.S. Department of Agriculture, Forest Service, Pacific Southwest Research Station, Vallejo, CA 94592

Sarah Hart, Colorado State University, Department of Forest and Rangeland Stewardship, Fort Collins, CO 80521

Crystal S. Homicz, PhD Candidate, University of California, Department of Entomology and Nematology, Davis, CA 95616

Christel C. Kern, Research Forester, U.S. Department of Agriculture, Forest Service, Northern Research Station, Rhinelander, WI 54501

Simone Lim-Hing, Assistant Research Professor, North Carolina State University, Department of Forestry and Environmental Resources, Raleigh, NC 27695

Qingqing Liu, Graduate Research Assistant, Shanxi Normal University, School of Life Sciences, Taiyuan 030031, China

Xiaoyu Liu, Graduate Research Assistant, Shanxi Normal University, School of Life Sciences, Taiyuan 030031, China

Zhiping Liu, Graduate Research Assistant, Shanxi Normal University, School of Life Sciences, Taiyuan 030031, China

Leif A. Mortenson, Ecologist, U.S. Department of Agriculture, Forest Service, Pacific Southwest Research Station, Placerville, CA 95667

Karun Pandit, Assistant Research Professor, North Carolina State University, Department of Forestry and Environmental Resources, Raleigh, NC 27695

Sandra Rideout-Hanzak, Professor of Fire Ecology and Restoration, Research Scientist, Texas A&M University-Kingsville, Department of Animal, Rangeland, and Wildlife Sciences, Caesar Kleberg Wildlife Research Institute, Kingsville, TX 78363

Justin B. Runyon, Research Entomologist, U.S. Department of Agriculture, Forest Service, Rocky Mountain Research Station, Bozeman, MT 59717

Paul C. Stoy, University of Wisconsin, Department of Biological Systems Engineering, Madison, WI 53706

Haibin Su, Professor of Geography, Texas A&M University-Kingsville, Department of Physics and Geosciences, Kingsville, TX 78363

Mukti Ram Subedi, Graduate Research Assistant, Texas A&M University-Kingsville, Department of Biological and Health Sciences, Kingsville, TX 78363; Postdoctoral Associate, University of Georgia, Warnell School of Forestry and Natural Resources, Athens, GA 30602

Anne Timm, U.S. Department of Agriculture, Forest Service, Northern Research Station, Baltimore, MD 21228

Amy M. Trowbridge, University of Wisconsin, Department of Forest and Wildlife Ecology, Madison, WI 53706

Angela Waupochick, University of Wisconsin, Nelson Institute for Environmental Studies, Madison, WI 53706

Justin P. Williams, Remote Sensing Program Manager, U.S. Department of Agriculture, Forest Service, Eastern Region, Forest Health Protection, Durham, NH 03824

Weimin Xi, Professor of Biology, Senior Ecologist, Texas A&M University-Kingsville, Department of Biological and Health Sciences, Kingsville, TX 78363

Ming Yan, Associate Professor, Shanxi Normal University, School of Life Sciences, Taiyuan 030031, China

Lim-Hing, S.; Pandit, K., eds. 2026. Forest Health Monitoring: Evaluation Monitoring project summaries 2024. Gen. Tech. Rep. WO-109a. Washington, DC: U.S. Department of Agriculture, Forest Service. 51 p. https://doi.org/10.2737/WO-GTR-109a.

Evaluation Monitoring is a component of the Forest Health Monitoring program of the U.S. Department of Agriculture, Forest Service. The overarching goal of Evaluation Monitoring projects is to assess changes in forest health, often at a finer scale than standard monitoring activities. After a project is completed, investigators provide an overview of the scope, methods, and findings. Previous Evaluation Monitoring project summaries are searchable on the Forest Health Monitoring website. This report includes summaries of four recently completed projects: "Using Climate and Remote Sensing Data to Map Current and Future Effects of Balsam Woolly Adelgid in Northern Utah;" "The California Tree Mortality Network: Monitoring Forest Change Following Extreme Drought in the Central and Southern Sierra Nevada, CA;" "Establishing a Monitoring System of Emerald Ash Borer Invasion Impacts on Tribal Black Ash Wetlands;" and "The Impacts of an Exceptional Drought on Forests in Eastern Texas: Disparities in Tree Mortality, Biomass Loss, and Decrease in the Carbon Sink Capacity."

Keywords—Balsam woolly adelgid, bark beetles, California Tree Mortality Network, climate modeling, drought, emerald ash borer, evapotranspiration, hydrological function, tree mortality, wetlands

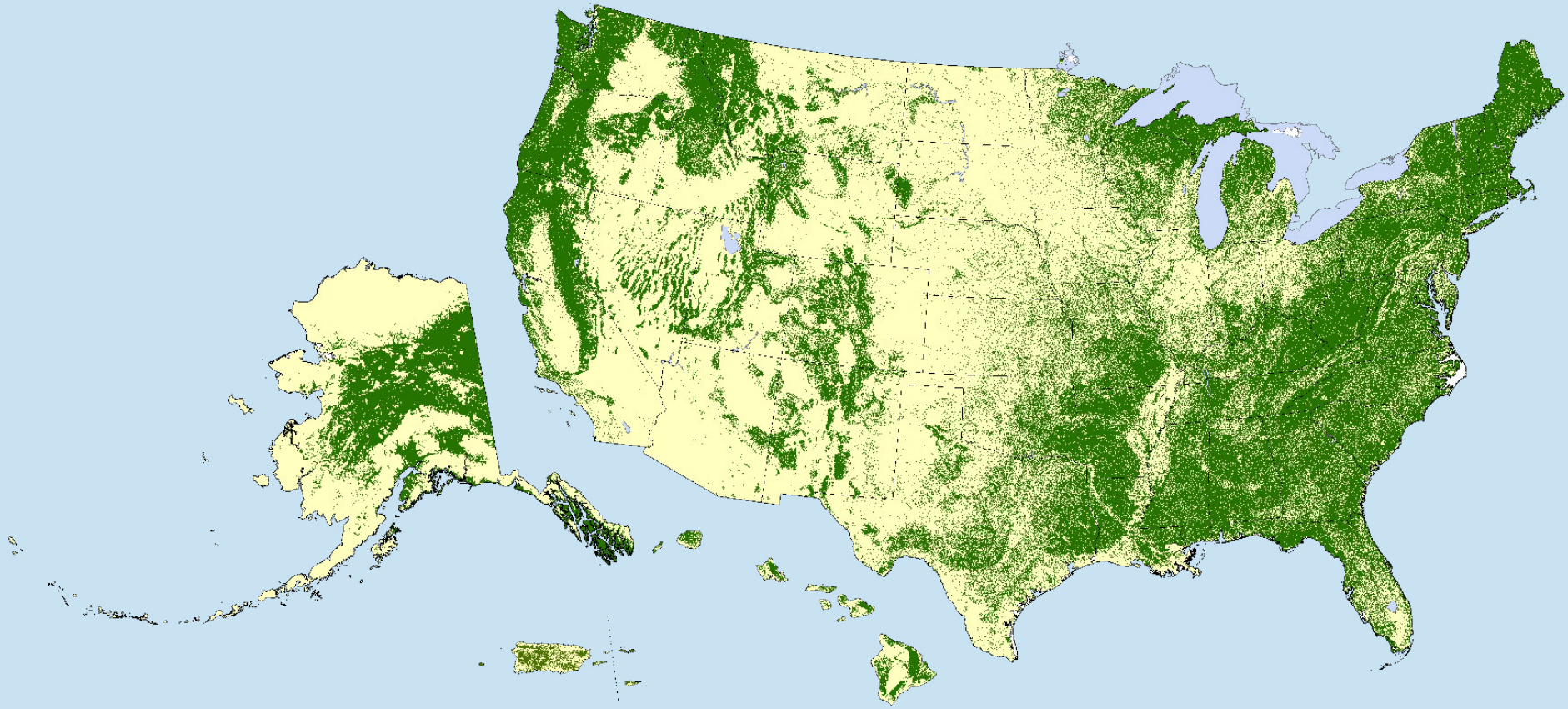

In accordance with Federal civil rights law and U.S. Department of Agriculture (USDA) civil rights regulations and policies, the USDA, its Agencies, offices, and employees, and institutions participating in or administering USDA programs are prohibited from discriminating based on race, color, national origin, religion, sex, disability, age, marital status, family/parental status, income derived from a public assistance program, political beliefs, or reprisal or retaliation for prior civil rights activity, in any program or activity conducted or funded by USDA (not all bases apply to all programs). Remedies and complaint filing deadlines vary by program or incident.

Persons with disabilities who require alternative means of communication for program information (e.g., Braille, large print, audiotape, American Sign Language, etc.) should contact the State or local Agency that administers the program or contact USDA through the Telecommunications Relay Service at 711 (voice and TTY). Additionally, program information may be made available in languages other than English.

To file a program discrimination complaint, complete the USDA Program Discrimination Complaint Form, AD-3027, found online at How to File a Program Discrimination Complaint and at any USDA office or write a letter addressed to USDA and provide in the letter all of the information requested in the form. To request a copy of the complaint form, call (866) 632-9992. Submit your completed form or letter to USDA by: (1) mail: U.S. Department of Agriculture, Office of the Assistant Secretary for Civil Rights, 1400 Independence Avenue, SW, Mail Stop 9410, Washington, D.C. 20250-9410; (2) fax: (202) 690-7442; or (3) email: program.intake@usda.gov.

USDA is an equal opportunity provider, employer, and lender.